Tyre/road contact stresses measured and modelled in three coordinate directions

September 2009

R. A. Douglas

Golder Associates Ltd, Mississauga, Ontario, Canada

NZ Transport Agency research report 384

ISBN 978-0-478-35217-7 (print)
ISBN 978-0-478-35216-0 (electronic)
ISSN 1173-3756 (print)
ISSN 1173-3764 (electronic)

NZ Transport Agency
Private Bag 6995, Wellington 6141, New Zealand
Telephone 64-4-894 5400; facsimile 64-4 894 6100
research@nzta.govt.nz
www.nzta.govt.nz

Douglas, RA (2009) Tyre/road contact stresses measured and modelled in three coordinate directions. *NZ Transport Agency research report 384*. 96pp.

Keywords: CAPTIF, contact stresses, full-scale testing, numerical modelling, pavement performance, pavement response, rutting, thin pavements, tyre contact patch, tyre scuffing

An important note for the reader

The NZ Transport Agency is a Crown entity established under the Land Transport Management Act 2003. The objective of the Agency is to undertake its functions in a way that contributes to an affordable, integrated, safe, responsive and sustainable land transport system. Each year, the NZ Transport Agency funds innovative and relevant research that contributes to this objective.

The views expressed in research reports are the outcomes of the independent research, and should not be regarded as being the opinion or responsibility of the NZ Transport Agency. The material contained in the reports should not be construed in any way as policy adopted by the NZ Transport Agency or indeed any agency of the NZ Government. The reports may, however, be used by NZ Government agencies as a reference in the development of policy.

While research reports are believed to be correct at the time of their preparation, the NZ Transport Agency and agents involved in their preparation and publication do not accept any liability for use of the research. People using the research, whether directly or indirectly, should apply and rely on their own skill and judgment. They should not rely on the contents of the research reports in isolation from other sources of advice and information. If necessary, they should seek appropriate legal or other expert advice.

Acknowledgements

Engineering research projects often rely very heavily on the competence and willingness of technical staff involved. This project benefited greatly from the solid expertise and enthusiasm of the technical staff at the Transit NZ (now NZ Transport Agency) CAPTIF lab, Alan Fussell and Frank Adams, together with Frank Greenslade in the Department of Civil Engineering, University of Canterbury, Christchurch. The support of Rui Oliveira of Golder Associates, Mississauga, Ontario, Canada lab was much appreciated.

Terms and abbreviations

CTI	Central tyre inflation (system): a system on a truck to permit the operator to vary the inflation pressure of the tyres as the truck drives along
Dual tyres	Two tyres closely spaced side by side on a wheel
FEM	Finite element method: a numerical method for estimating stresses, strains and displacements in pavements or soil masses
NZ Transport Agency	The NZ Transport Agency (NZTA) was formally established on 1 August 2008, combining the functions and expertise of Land Transport NZ and Transit NZ.
Pavement performance	The long-term behaviour of the pavement over time, often measured in terms of rut development
Pavement response	The reaction of the pavement, in terms of stresses, strains and displacements, to loading
RLT	Repeated load triaxial test (on a base aggregate sample)
Test designations	These are given as, for example, S40690, denoting a single tyre, with a wheel load of 40kN, and an inflation pressure of 690kPa
Wheel load	Half the axle load, whether the axle is equipped with single or dual tyres

Contents

Executive summary

The pavement engineering community sees the increased use of marginal pavement materials as a key factor for more sustainable use of natural resources; however, successful use of alternative materials requires the ability to reliably model pavement response and performance. In turn, these models depend on the accurate portrayal of the tyre/road surface contact stress distributions.

The goal of the project was to enable the improvement of the modelling of pavement response and performance through the measurement of full-scale contact stress distributions in all three of the coordinate directions, vertical, longitudinal and transverse.

Project objectives were to:

- measure the contact stresses imposed by various tyre types, inflation pressures and wheel configurations, to identify the more benign combinations
- use the measured data in numerical models of the response of pavements: modelling is currently limited by the quality of input loading data available
- use the measured data in analyses of the rutting of pavements
- support existing research into the scuffing effects of various axle combinations which currently relies on tyre forces as inputs.

An apparatus to measure contact stresses was designed and constructed. It comprised 25 strain-gauged pins, 5mm square, housed in a strong steel box, mounted flush with the pavement surface. Protruding 1mm above the surface of the box, the pins sensed the vertical, longitudinal and transverse contact forces imposed on them by the tyres.

Load testing was carried out in the CAPTIF full-scale, indoor testing facility maintained by Transit NZ (now NZ Transport Agency) in Christchurch. Test configurations included single tyres and dual tyres, wheel loads of 40 and 50kN, and inflation pressures of 280, 550 and 690kPa.

Typical results for the vertical pin loads agreed with patterns seen in the literature. However, this was not the case for the longitudinal and transverse pin loads. The differences were thought to be due to tyre scuffing occurring on the circular test track.

Pin loads were used to derive contact stress distributions input to a finite element numerical model of pavement response developed by the Technische Universitaet Dresden. Comparisons were made to determine if using these non-uniform contact stresses gave rise to different elastic pavement stresses, strains and displacements, compared with the results obtained when a conventional uniformly distributed pressure was input as loading. In general, there were small but measurable differences. For single tyres, vertical stresses under the tyre at the top of the subgrade were 3% to 8% greater for the non-uniform contact stresses, peak vertical strains in the base were 16% to 20% greater, and vertical surface displacements were 5% to 8% greater.

The differences between the results for uniform and non-uniform contact stresses *were* significant, however, when the pavement performance, in terms of rutting predicted by a model developed by S Werkmeister at the Technische Universitaet, Dresden, was examined. For a typical New Zealand thin pavement, for the loadings assumed in the comparison, predicted rutting was approximately 25% greater at one million passes if the non-uniform contact stresses were input to the pavement performance model.

Objectives 2 and 3 above were achieved. Objectives 1 and 4 were not:

- The tyre-scuffing effect caused by the tyres running on the circular track confounded the results, making it impossible to compare the effects of tyre types, configurations, wheel loads and inflation pressures.
- To carry out research on scuffing effects properly came to be seen as beyond the scope of the project; however, a much clearer vision of what would be needed to address such research has been gained.

The report includes a comprehensive literature search covering the measurement of tyre contact stress, the use of measured contact stresses in numerical models of pavement response, current lines of research and conclusions. In addition, the full report on the numerical modelling is provided in the appendix.

All test results have been posted in a publicly available website: www.golder.com/Contact_Stress_Study

Abstract

To enable the improvement of the modelling of pavement response and performance, the measurement of full-scale tyre surface contact stress distributions in all three of the coordinate directions was undertaken. An apparatus comprising strain-gauged pins housed in a strong steel box, mounted flush with the pavement surface was built. The pins were designed to sense the contact forces imposed on them by the tyres.

A programme of full-scale load testing was carried out (single and dual tyres, wheel loads of 40 and 50kN, and inflation pressures of 280, 550 and 690kPa).

Typical results for the vertical pin loads agreed with patterns seen in the literature. However, this was not the case for the longitudinal and transverse pin loads.

Comparisons were made between pavement response predicted by a finite element model for two loading cases: (1) a uniformly distributed pressure on the tyre contact patch, and (2) the non-uniform contact stresses derived from the experimental results. Differences in pavement response were generally measurable but not great. The difference in pavement performance was significant.

The report includes a comprehensive literature search. All measured experimental results have been posted to a publicly available website.

1 Introduction

The pavement engineering community sees the increased use of recycled and marginal pavement materials as a key factor for more sustainable use of natural resources. However, successful use of alternative materials requires the ability to reliably model pavement response and performance. In turn, these models depend on the accurate portrayal of the tyre/road surface contact stress distributions. There is little high-quality measured data available on this subject. Thus the purpose of the project was to enable the improvement of the modelling of pavement response and performance through the measurement of full-scale tyre/road surface contact stress distributions in all three of the coordinate directions, vertical, longitudinal and transverse. To the author's knowledge, only a handful of other apparatuses capable of making these measurements exist world-wide, including one in South Africa (de Beer et al 1997) and one in Northern Ireland (Douglas et al 2000). The research was designed to extend work on contact forces being undertaken in Australia with a large plate apparatus.

Project objectives were to:

- measure the contact stresses imposed by various tyre types, inflation pressures and wheel configurations, to identify the more benign combinations, particularly with reference to their use on thin seals and thin asphalt pavements
- use the measured data in numerical models of the response of pavements: models have reached a high degree of sophistication, but are currently limited by the input loading data available
- use the measured data in analyses of the rutting of pavements
- support existing research into the scuffing effects of various axle combinations which currently relies on tyre forces as inputs, and could benefit from the measurement of contact stress distributions.

At the time the project's proposal was submitted to the then-Land Transport NZ (now the NZ Transport Agency), an apparatus designed to measure the contact stresses was partially fabricated. A steel box approximately 600mm long had been constructed and equipped with one strain-gauged pin, protruding 1mm above the box's top plate (figures 1.1 and 1.2). Preliminary data had been collected, which consisted of traces of the vertical, longitudinal and transverse forces exerted on the tip of the pin when driven over by a car (figure 1.3).

Figure 1.1 Trial of single sensing pin

Figure 1.2 Pin is in the third hole from the right

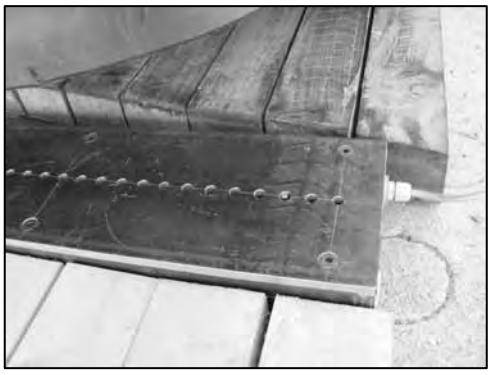

Figure 1.3 Preliminary output from apparatus: loads on pin under tyre edge rib, 195/70R14 tyres, inflation pressure approximately 210kPa, mounted on the passenger car shown in figure 1.1 (a) vertical load, (b) longitudinal load, (c) transverse load on pin

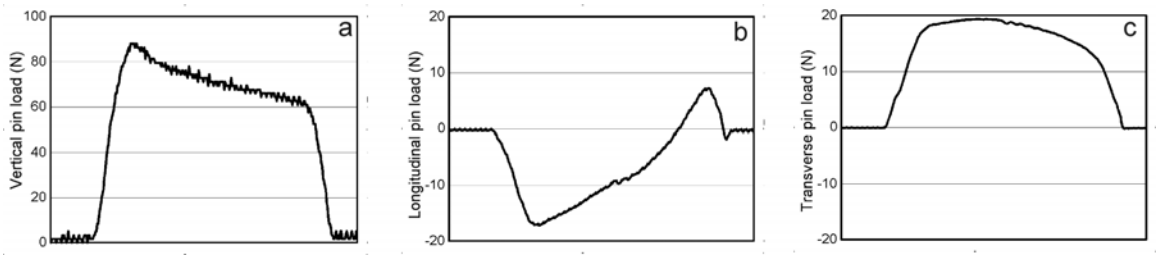

Work on the project first began at the University of Canterbury, but the author subsequently resigned his position at the University and moved to Golder Associates Ltd, in Mississauga, Ontario, Canada. Land Transport NZ agreed to move the project to Golder Associates, given that the research plan and personnel were to remain as had originally been proposed. The author used Golder Associates' Mississauga clean laboratory for the strain-gauged pin fabrication, otherwise all work took place as originally planned, in Christchurch at the University of Canterbury and the Transit NZ (now NZ Transport Agency) CAPTIF facility, and at the Technische Universitaet Dresden, the premises of the numerical modeller.

An early component of the work was a review of the literature, which is given in the following section. After the presentation of the literature review, a description of the apparatus, a description of the load testing, an analysis of the data, a discussion and conclusions are presented. The report finishes with a list of recommendations for further research.

An internal report was written in association with the project and is included as the appendix to this report.

2 Literature review

2.1 Introduction

This review of the literature provides the background to the present research on the modelling of flexible pavement response and performance, enhanced by the input of measured – rather than assumed – tyre/road surface contact stresses. Contact stress distributions are discussed first, followed by discussion of the technologies used to measure contact stresses and examples of the use of measured stresses in numerical modelling of pavement behaviour.

2.2 Tyre/road surface contact stress distributions

(with material extracted from Douglas et al (2000)

Lippmann (1985) indicated that vertical contact stresses under tyres should be expected to be non-uniform, as illustrated in figure 2.1 for a tyre of low inflation pressure. The vertical component of the inflation pressure acting on the bulging sidewalls beyond the edge of the tread is supported by increased contact stress under the outer tread rib and by bending stresses in the tyre carcass. Toward the centre of the tread, the tyre acts more like a membrane, with the inflation pressure being resisted by an approximately equal contact stress beneath the tyre. For tyres with high inflation pressure, the contact stress is higher in the centre of the tread than at the sidewalls. Marshek et al (1986) and de Beer et al (1997) provided experimental evidence of the non-uniformity of the vertical stress distribution over the contact patch.

Figure 2.1 Cross section of tyre with low inflation pressure under heavy load (after Lippmann (1985))

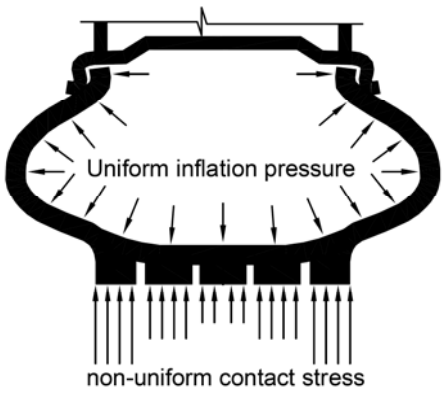

The tread grooves separate zones of widely varying vertical contact stress (Marshek et al 1986). The non-uniformity of vertical contact stress is partly due to the bending stiffness of the tyre carcass; this implies that the vertical contact stress distribution will be dependent on tyre design (Tielking and Roberts 1987). Also, tread imperfections and mould marks can significantly influence measured vertical contact stresses (Howell et al 1985).

It should be noted that the vehicle speed has almost no impact on vertical contact stresses; static vertical contact stresses are about equal to dynamic vertical contact stresses (Tielking and Roberts 1987). On the other hand, longitudinal contact stresses *are* affected by vehicle speed (Tielking and Roberts 1987). The formerly curved tread surface of a stationary tyre sitting on pavement is forced to become planar within the contact patch (Tielking and Roberts 1987). Friction between the tread face

and the road surface develops tangential stresses (figure 2.2(a)) directed on the road surface toward the centre of the contact patch. When the tyre is rolling freely, longitudinal shear stresses develop in the middle of the contact patch (figure 2.2(b)), resulting in a double reversal of the longitudinal stresses from the leading edge to the trailing edge of the contact patch (Lippmann 1985; Tielking and Roberts 1987; Siegfried 1998).

Figure 2.2 Plan view of horizontal contact stresses imposed on the road surface within the tyre contact patch: (a) static tyre and (b) freely rolling tyre (after Tielking and Roberts (1987))

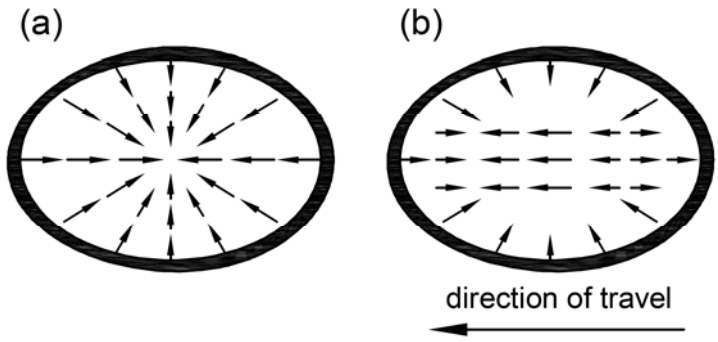

As a point on the outer rib of the tyre rolls into the contact patch, it is pushed laterally toward the centre, and therefore transverse stresses also develop within the contact patch (Tielking and Roberts 1987). Longitudinal and transverse contact stresses are affected by tyre construction (radial or bias ply), with transverse shear stresses being less for radial tyres (Tielking and Roberts 1987).

2.3 A seminal publication

Two committees (E-17, Committee on Travelled Surface Characteristics, and F-9, Tires) of the American Society for Testing and Materials (ASTM) convened a symposium, The Tire Pavement Interface, in Columbus Ohio, 5–6 June 1985 (ASTM 1985). The 11 papers listed in Table 2.1 were presented, encapsulating the state of the art at the time.

The papers by Howell et al (1985) and Lippman (1985) are particularly relevant to the present research, and are discussed in greater detail in this literature review.

2.4 The measurement of tyre contact stress

(with material extracted from Douglas et al 2000)

Researchers have approached the concept of contact stresses beneath tyres from a number of points of view, including terramechanics, tyre design and pavement design. Static testing and, more recently, dynamic testing have been performed.

Early interest is recorded in a paper presented by Eckels (1929), who used an apparatus dependent on springs and dial gauges (figure 2.3) to measure contact pressures, averaged across the width of the tyre, for solid and pneumatic tyres and ‘cushion tyres’. The research appeared to be an end in itself, with no reference made to the impact of contact stresses on pavement design.

Table 2.1 Papers presented at ASTM's 1985 symposium, The Tire Pavement Interface (ASTM 1985)

The traction connection	
Henry, JJ	*Tire wet-pavement traction measurement: a state-of-the-art review*
Horne, WB, TJ Yager and DL Ivey	*Recent studies to investigate effects of tire footprint aspect ratio on dynamic hydroplaning speed*
Wambold, JC, JJ Henry and RR Hegmon	*Skid resistance of wet-weather accident sites*
Whitehurst, EA and JB Neuhardt	*Time-history performance of reference surfaces*
Lenke, LR and RA Graul	*Development of runway rubber removal specifications using friction measurements and surface texture for control*
The interfacial stresses, motions and wear	
Lippman, SA	*Effects of tire structure and operating conditions on the distribution of stress between the tread and the road*
Howell, WE, SE Perez and WA Vogler	*Aircraft tire footprint forces*
Veith, AG	*The most complex tire-pavement interaction: tire wear*
Shepherd, WK	*Diagonal wear predicted by a simple wear model*
Pottinger, MG, KD Marshall, JM Lawther and DB Thrasher	*A review of tire pavement interaction induced noise and vibration*
McQuirt, JE, EB Spangler and WJ Kelly	*Use of the inertial profilometer in the Ohio DOT Pavement Management System*

Figure 2.3 Early apparatus to measure vertical contact pressures (Eckels 1929)

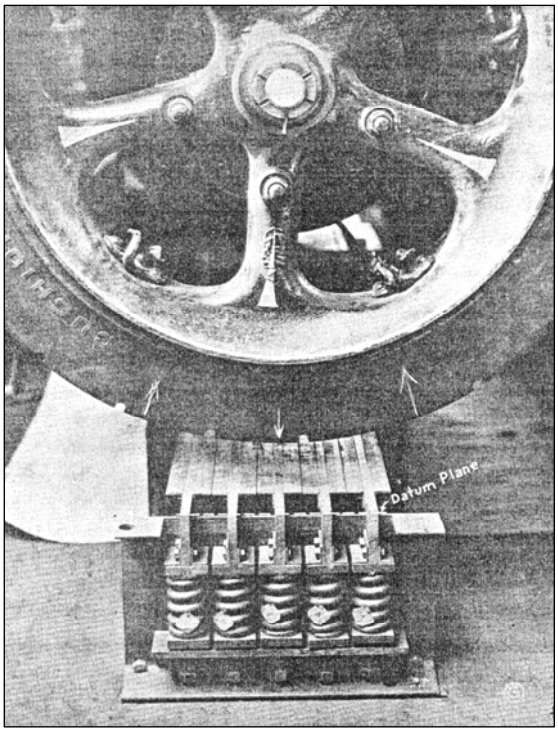

Forty years elapsed until O'Neil (1969) carried out static tests on tyres mounted in a load frame, bearing on an array of nylon pins connected to proving rings. Some time later, Howell et al (1985) investigated contact stresses for aircraft tyres by loading a tyre in a test frame. Static contact stresses were sensed by 12.7mm square strain-gauged elements mounted in a platen suspended beneath the tyre by cables.

Lippmann (1985) studied dynamic interface stresses by monitoring the output of a single triaxial sensor with a 5mm square face. Over successive tests, the sensor was moved to different lateral positions, to record the stresses at various locations across the tread face. It is important to note in Lippmann's study that the tyre deflection, rather than the tyre load, was controlled. Thus, the load for any particular test was unknown.

Marshek et al (1986) measured static contact stresses using a novel arrangement of pressure sensitive film coated with microscopic ink bubbles, and a photocell for subsequently reading the intensity of the tiny blots left by the ink bubbles burst under the pressure of the tyre.

To measure the ground contact stresses imposed by forestry skidder tyres, Smith et al (1990) placed an instrument *in the tyre* rather than in the ground over which the skidder ran. A hydraulic pressure transducer embedded in a lug of the skidder tyre detected pressure exerted on a piston protruding from the tyre lug, as it contacted the ground.

Tielking and Abraham (1994) measured static contact stresses under a tyre in a load test frame using an array of 10 triaxial load sensors. The sensor array could be moved small increments laterally between tests, to permit the collection of the complete stress profile across the tyre tread.

Liu (1992) and subsequently Siegfried (1998) used the apparatus described in Douglas et al (2000) to assess static and dynamic stresses under both passenger car and truck tyres.

An array of 21 triaxial strain-gauged pins was used by de Beer et al (1997) to measure dynamic stresses under a wide range of tyres. Attention was paid to the texture of the surface around the sensor array.

Table 2.2 provides the details of the research outlined above. When reviewing and comparing the literature, one must be careful to note the particulars of the various research projects, including:

- whether bias ply or radial ply tyres were used
- the nature of the surface on which the tyre travelled
- whether static or dynamic tests were performed
- whether the tyre was rolling freely or was powered
- whether stresses were reported as those acting on the sensors or those acting on the tread face
- which coordinate directions were assumed as 'positive'.

Table 2.2 Summary of studies to 1999 (Douglas et al 2000)

	Test: static / dynamic	Tyre	Tyre load (kN)	Inflation pressure (kN/m²)
O'Neil (1969), cited in Marshek et al (1986)	Static	Assumed bias ply	na	na
Howell et al (1985)	Static	40×14 Type VII 28-ply aircraft tyre	9–133	970–1170
Lipmann (1985)	Dynamic	P205/75R14	≈ 5 (controlled by axle height)	210–410
Marshek et al (1986)	Static	10–20 bias ply	20-24	520–760
Liu (1992)	Static	175/70SR80S	4	210
Liu (1992)	Static	8.25R20 14 ply	9–21	480–690
Liu (1992)	Dynamic	??	3–4	210?
Tielking and Abraham (1994)	Static	11R24.5 (smooth)	22–29	620–720
Tielking and Abraham (1994)	Static	11R24.5 (treaded)	27–36	550–720
de Beer et al (1997)	Dynamic	11.00×20 14 ply bias (smooth)	20–50	420–720
de Beer et al (1997)	Dynamic	11.00×20 14 ply bias (smooth)	10–40	420–720
de Beer et al (1997)	Dynamic	46×16 30 ply aircraft tyre	20–50	1450
de Beer et al (1997)	Dynamic	315/80R22.5	20–100	500–1000
de Beer et al (1997)	Dynamic	425/65R22.5	25–100	500–1100
de Beer et al (1997)	Dynamic	425/65R160 wide base	25–100	500–1100
Tielking and Abraham (1994)	Static	385/65R22.5 (treaded, wide base	27–40	660–900
Siegfried (1998)	Static	175/70R13	2–4	100–170
Siegfried (1998)	Static	8.25R20 14 ply	10–20	280–550
Siegfried (1998)	Dynamic	8.25R20 14 ply	4–7	280–550
Woodside et al (1999)	Dynamic	8.25R20 14 ply	5–24	100–690

The ranges of tyre load and inflation pressure for each of the projects listed in table 2.2 are plotted in figure 2.4. Ranges tended to be grouped around those appropriate for automobile tyres (tyre loads 3–5kN) or trucks (tyre loads 10–40kN), with the addition of two studies of aircraft tyres. An absence of studies where dynamic contact stresses for heavy tyre loads (>25kN) combined with low inflation pressures (<300kN/m2) is observed (Douglas et al (2000).

Figure 2.4 Ranges of tyre load vs inflation pressure for studies of contact stresses: (a) static and (b) dynamic (Douglas et al 2000)

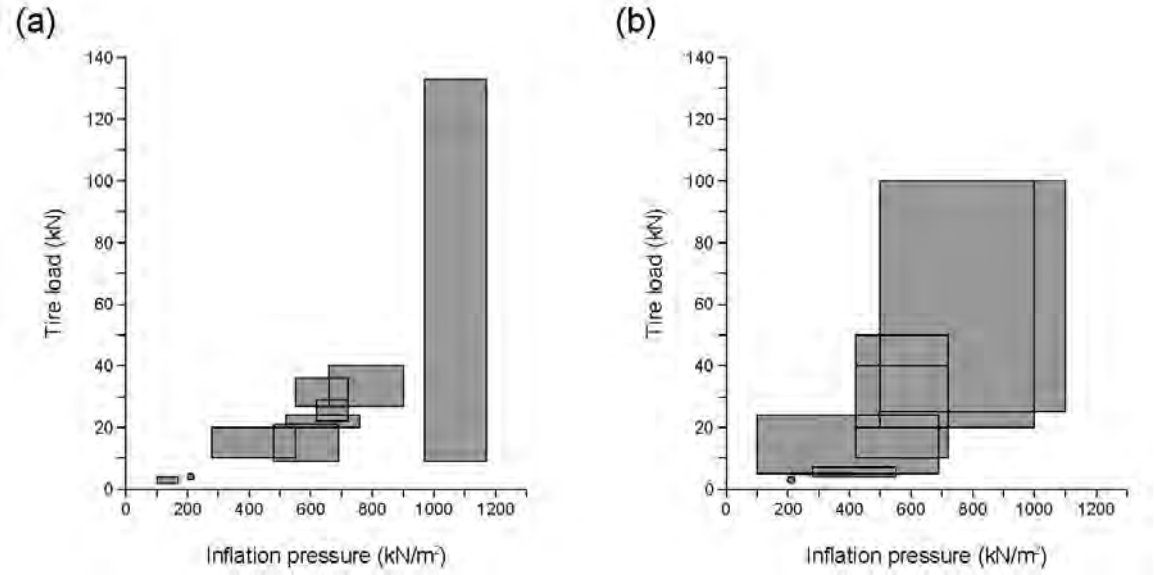

2.5 Developments in the technology for measuring contact stresses

Contact stress apparatuses currently in use rely on strain-gauge technology. Electrical resistance strain gauges are cemented to small steel pins, fixed in the vertical position as vertical cantilevers, with the top end flush with a base plate over which the tyre is run. The strain gauges are arranged to detect the axial load in the pin caused by the vertical tyre pressure, and the bending in the pin caused by longitudinal and transverse shears imposed by the tyre on the end of the pin.

Roque et al (2000) cautioned that instruments embedded in road structures are necessarily founded on *rigid* bases, whereas flexible pavements are, by definition not rigid. Thus, the experimental boundary conditions presented to tyres running over sensing arrays are not the same as for a real pavement. Roque et al (2000) conducted a finite element study, and fortunately determined that generally the vertical and lateral tyre contact stresses measured on rigid foundations accurately represented the same contact stresses for the same tyre on typical asphalt structures. While they noted some differences for thin pavements (50mm), they concluded that the contact stresses measured by apparatuses with rigid foundations – those currently in use – appeared to be suitable for predicting the response and performance of real pavements (Roque et al 2000). This has important implications for the current research.

2.6 Applications of contact stress research: supporting numerical model studies

The recent literature is replete with publications detailing the *uses* of contact stress measurement. Pavement researchers have waited some time to be able to use *realistic* surface stresses in their numerical models of pavement response and performance. It is ironic that the models have become highly sophisticated, yet until very recent times have relied on relatively crude assumptions about the

stresses imposed on the pavement surface by the tyre. A representative handful of the publications is outlined here.

Weissman (1999) used actual contact stress measurements provided by others in a linear layered elastic analysis of pavements and found that the real stresses, imposed over the real contact patch shape led to considerably larger stresses in the pavement relative to those generated by the imposition of a uniform pressure.

Drakos et al (2001) were interested in near-surface pavement rutting. They used measured tyre / pavement contact stresses to determine the effects of tyre structure, load and inflation pressure on the contact stress distribution. The loads were then input to the elastic layer program BISAR to predict the pavement's response. Near-surface tension and high shear stresses were predicted in the pavement by the analysis. These were thought to provide an explanation for the mechanics of near-surface rutting.

The effect of non-uniform contact stress distributions on permanent deformation profiles in asphalt pavements was examined by Park et al (2005a). A three-dimensional finite element program that used non-uniform contact stresses measured at WesTrack showed that the distribution of stresses influenced pavement response. Their finite element model was able to simulate the measured permanent deformation profiles. In other work (Park et al 2005b), a three-dimensional finite element program using measured contact stresses predicted pavement strains and estimated pavement service life.

Prozzi and Luo (2005) input measured contact stresses to CIRCLY, a long-established layered pavement analysis program, to predict pavement response. When compared with the results obtained for uniform contact stresses acting over a circular contact patch, the uniform stress approach yielded similar compressive strains on the top of the subgrade, and conservative (higher values) estimates of tensile strains at the bottom of the asphalt layer.

A model reported in Siddharthan et al (2002) called 3D-MOVE, first devised to investigate the differences in pavement response for uniform and non-uniform contact stresses, was subsequently used to evaluate the impacts on pavements of very heavy agricultural equipment with very large tyres (Siddharthan et al 2005).

Machemehl et al (2005) criticised the common use of uniform pressures on circular contact patches in pavement analyses. The pavement stresses and strains generated by this loading condition were compared to the strains generated by measured stresses, using an elastic multilayer analysis program. It was found that for both thick and thin asphaltic pavements, the tensile strains at the bottom of the asphalt layer and the stresses near the pavement surface were both significantly dependent on the contact stress distribution assumed in the analysis. However, especially for the thick pavements, the assumed contact stress distribution had little effect on the vertical strains at the top of the subgrade. This concurs with the finding of earlier work done on unsealed, unbound pavements (Douglas 1997a; Douglas 1997b)

Wang and Machemehl (2006) extended the work of Machemehl et al (2005), and found that the traditional loading (uniform pressure, circular contact patch) input to a multilayer program tended to overestimate the horizontal tensile strains (agreeing with the findings of Prozzi and Luo (2005)) and underestimate the vertical compressive strains at the top of the subgrade, when compared with a finite element analysis using measured contact stresses. The more sophisticated analysis indicated that increased tyre pressure resulted in greater pavement cracking and rutting, and that inflation pressure also influenced the shape of ruts (Wang and Machemehl, 2006).

2.7 Current lines of research

There are two systems for measuring contact stresses most commonly referred to in the literature.

One was devised by de Beer in South Africa. It has supported research discussed in numerous reports, including: de Beer et al (1997), Weissman (1999), Machemehl et al (2005), Prozzi and Luo (2005), and Wang and Machemehl (2006). The general approach has been to use measured contact stresses to first verify numerical models, then predict pavement response and/or performance.

The other system was designed and built at the University of Ulster, Northern Ireland. A series of publications have come from its development, including: Liu (1992), Siegfried (1998), Woodside et al (1999), Douglas et al (2000), and Douglas et al (2003). This line of research has moved recently toward quantifying contact stresses, in order to determine the energy exerted on chip-sealed pavement surfaces, the concern being that there might be enough energy in low-inflation pressure cases to pluck chips from pavement surfaces.

The current research project has its roots in the Ulster work, and draws on the experiences gleaned from the use of the de Beer apparatus.

3 Apparatus

The first project objective was to measure the contact stresses imposed by various tyre types, inflation pressures and wheel configurations. An apparatus had to be fabricated to make the measurements.

The contact stress measurement apparatus consisted of a strong steel box 680 x 180 x 95 mm (L x W x H) enclosing 25 steel pins 5×5 mm square arranged as vertical cantilevers in a closely spaced row across the width of the intended tyre path (figures 1.1, 1.2, 3.1 and 3.2).

Figure 3.1 Contact stress measurement apparatus: strain-gauged pin (left) and steel box (right)

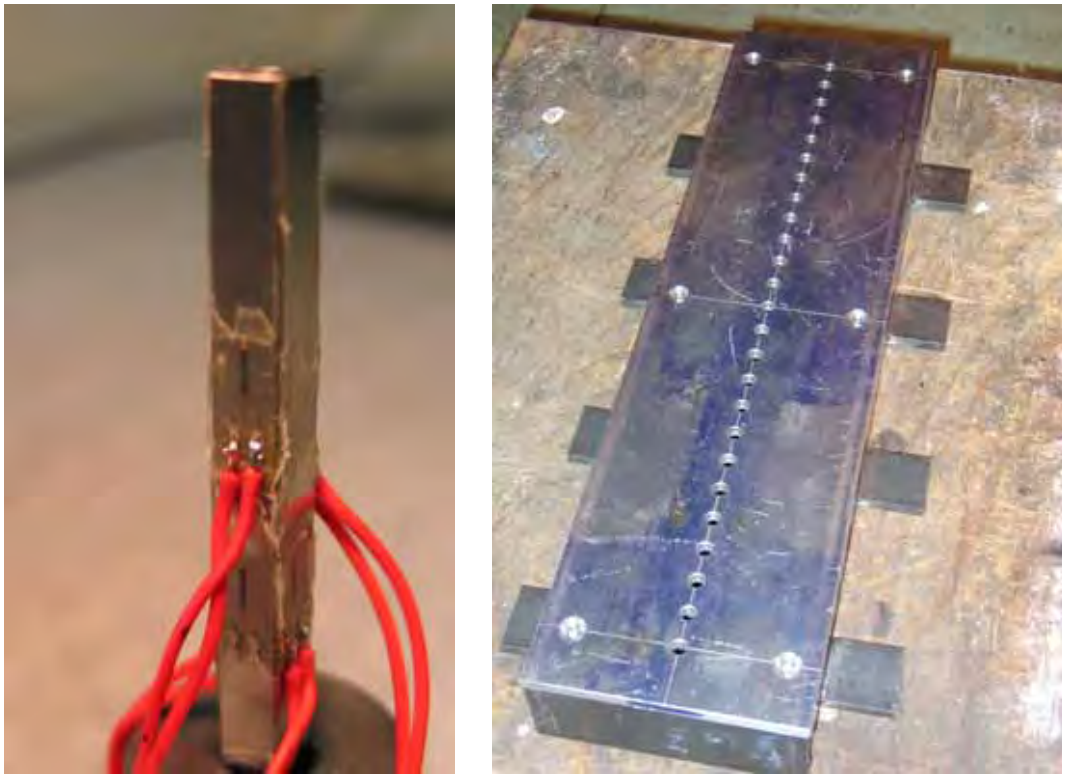

The pins protruded 1mm through holes in a surface plate over which the tyre rolled. They were equipped with electrical resistance strain gauges to measure vertical compression along their axes, and bending in the longitudinal and transverse directions, relative to the direction of travel of the tyre.

Each pin had six semi-conductor strain gauges installed in three pairs (figures 3.1 and 3.2). The gauges in each pair were arranged opposite one another, and wired into Wheatstone bridges to sense compression or bending in the pin, as appropriate for the pair. The pins were loaded with a series of dead weights (figure 3.3), the output recorded, and a linear regression derived in order to produce the required calibration coefficients. Each calibration was repeated at least three times. Bending calibrations were performed in opposite directions and the regression coefficients averaged.

Figure 3.2 (a) Strain gauge placement on pin. (b) Apparatus box

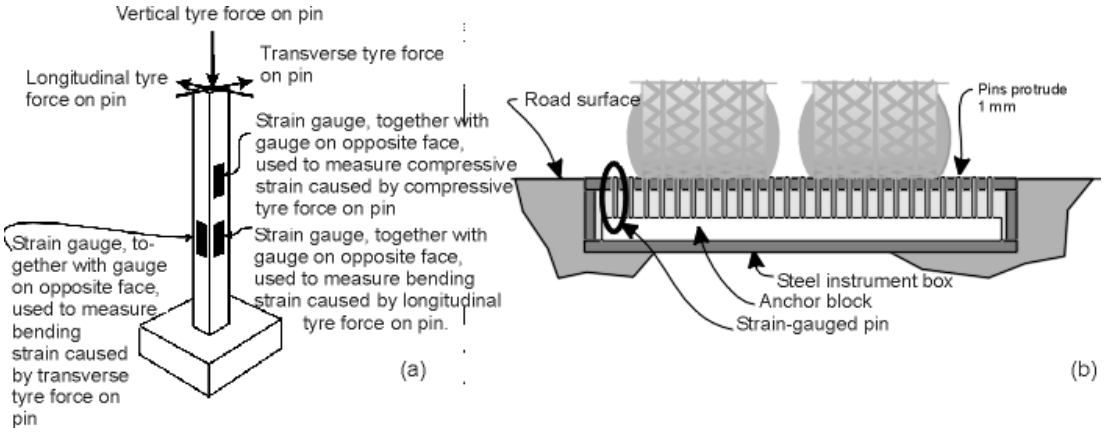

Figure 3.3 Calibration of strain-gauged pin

Figure 3.4 Installation of apparatus in CAPTIF full-scale test track

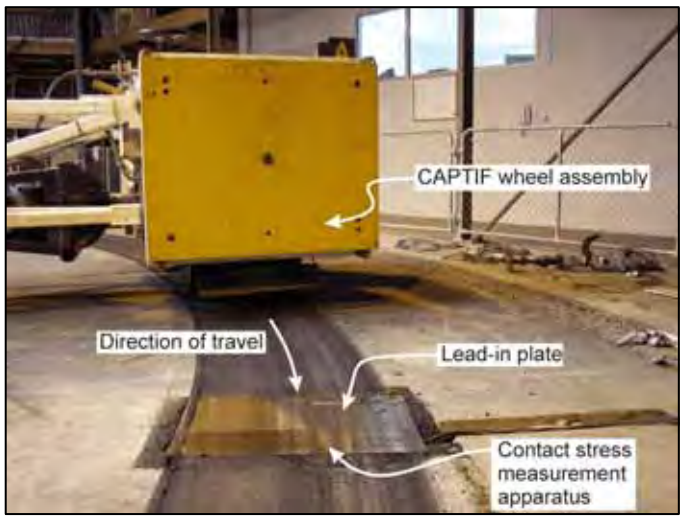

The apparatus was installed in a rectangular hole cut in the pavement of the CAPTIF full-scale indoor test track (figure 3.4). A lead-in plate was attached to the upstream side of the apparatus box to provide a smooth transition from pavement to apparatus cover plate.

The CAPTIF facility has two wheel assemblies at the ends of two opposing 9m long arms pivoted at the centre. The wheels are driven hydraulically on half-axles around a constant circle; the geometry of the device and track are such that forces across the width of the tyres and between the tyres may not be uniform. Wheel loads are applied with steel dead weight plates (the yellow square in figure 3.4).

A high-speed data acquisition system, capable of measuring any eight channels of data at a rate of 10,000 samples per second, was assembled. The data was acquired from four pins at a time, with four pins measured in compression and two pins in bending in both directions.

4 Full-scale tests and typical results

Table 4.1 shows the matrix of test parameters studied. Two wheel types, two wheel loads, and two or three inflation pressures were used in the full-scale load tests. At least five passes of the wheel were made at each combination of wheel load and inflation pressure.

Table 4.1 Load test combinations

Wheel type, tyre designation	Wheel load	Inflation pressure or deflection (kPa or %)
Dual tyres 295/80 R225 M840	40kN	690
		550
		20% (280 kPa)
Wide single 385/65 R225 R194		690
		550
	50kN	690
		550
Dual tyres 295/80 R225 M840		690
		550
		20% (280 kPa)

4.1 Typical results

Tyre patch lengths have been inferred from the data sampling rate and the speed of the tyre running around the test track. The approximate contact patch lengths are given in table 4.2.

Table 4.2 Approximate tyre contact patch lengths

Wheel type, tyre designation	Wheel load (kN)	Inflation pressure or deflection (kPa or %)	Approximate tyre contact patch length (mm)
Wide single 385/65 R225 R194	40	690	310
		550	330
	50	690	310
		550	360
Dual tyres 295/80 R225 M840	40	690	280
		20% (280 kPa)	370
	50	690	300
		20% (280 kPa)	410

Schematic plan views of the compressive, longitudinal and transverse pin loads are shown in figures 4.1 to 4.3, for all combinations of single wheel load and tyre inflation pressure tested. The plots show the pin load as a function of position within the tyre contact patch. Longitudinal distances were calculated based on the sensor sampling rate and tyre speed around the test track. Transverse

distances were multiples of the pin spacing of 25mm. The plots are not to scale: the longitudinal scale/transverse scale ratio is distorted.

Figure 4.1 Schematic plan view of compression pin loads for single tyres. Wheel loads (kN) and tyre inflation pressures (kPa) are shown for each plot (not to scale)

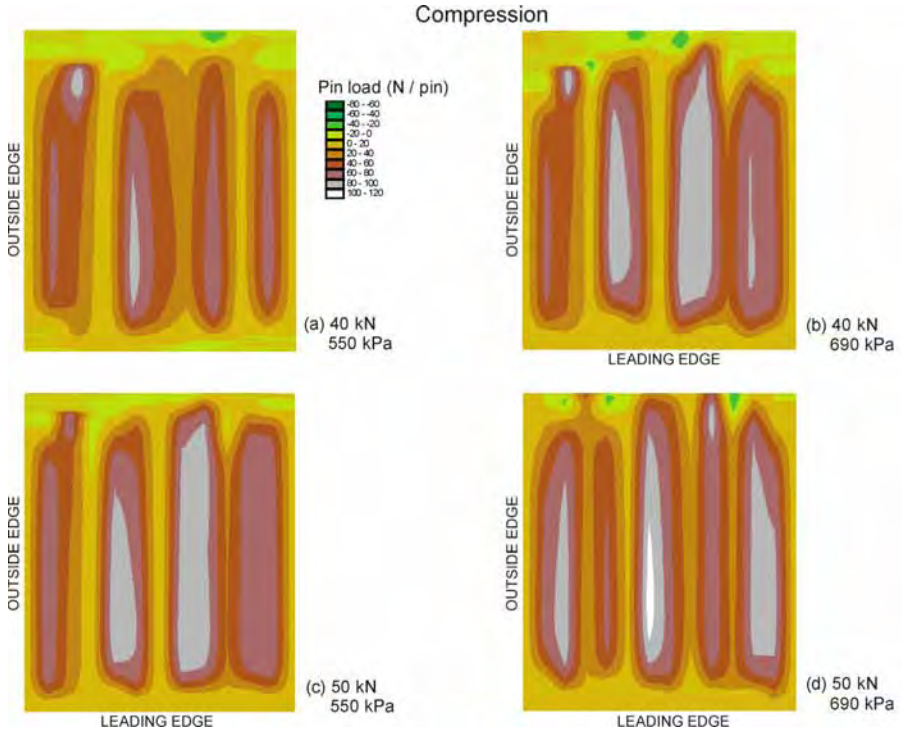

Figure 4.2 Schematic plan view of longitudinal pin loads for single tyres. Wheel loads (kN) and tyre inflation pressures (kPa) are shown for each plot (not to scale)

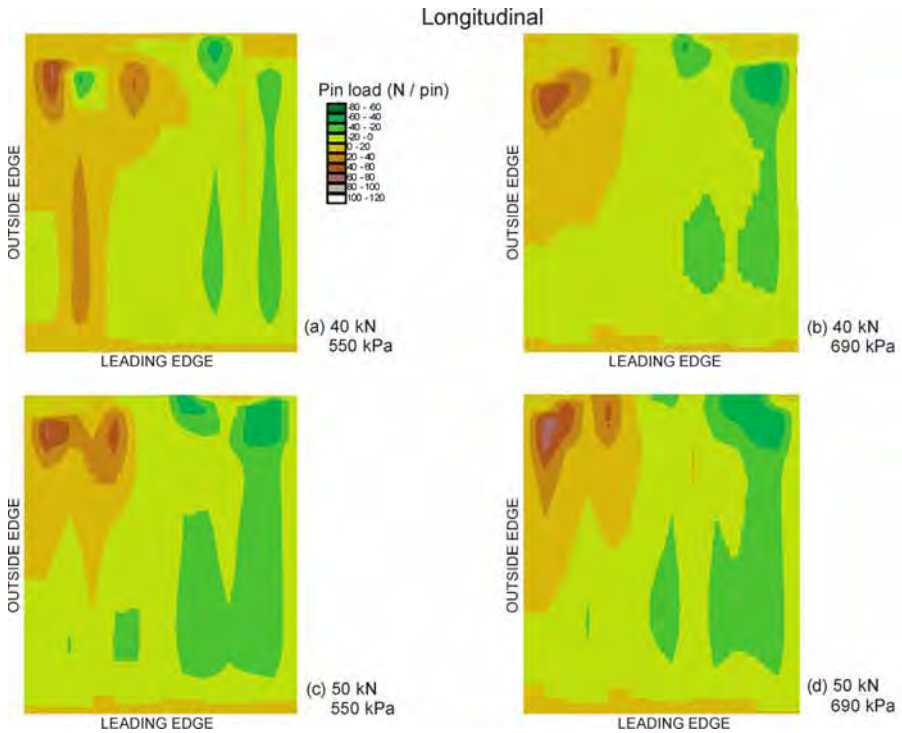

Figure 4.3 Schematic plan view of transverse pin loads for single tyres. Wheel loads (kN) and tyre inflation pressures (kPa) are shown for each plot (not to scale)

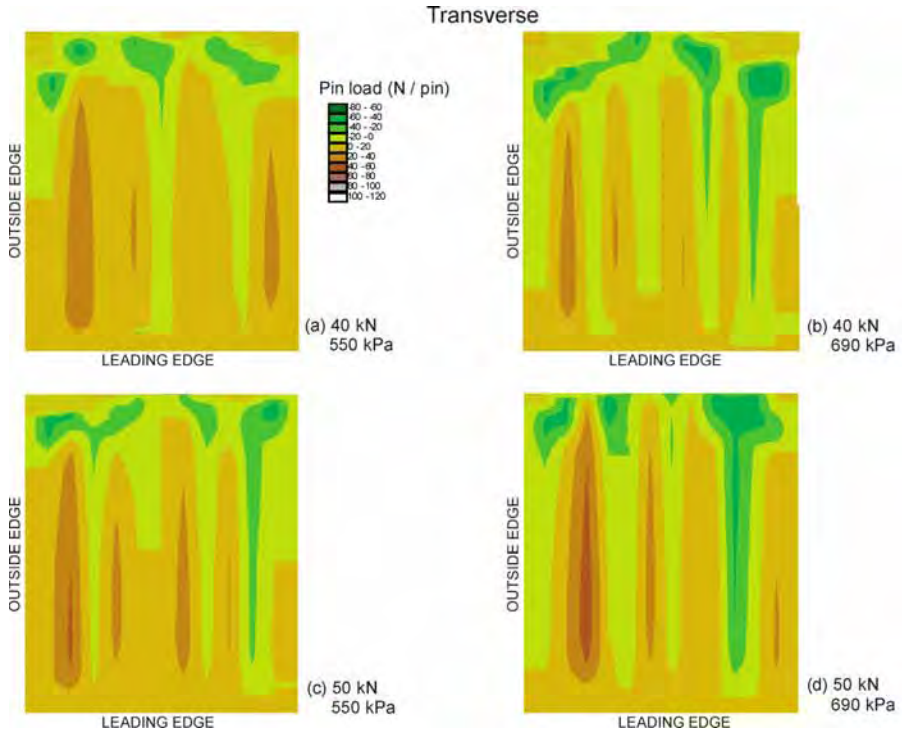

Figure 4.4 Schematic plan view of pin loads for dual tyres: wheel load 40kN, tyre inflation pressure 690kPa (not to scale)

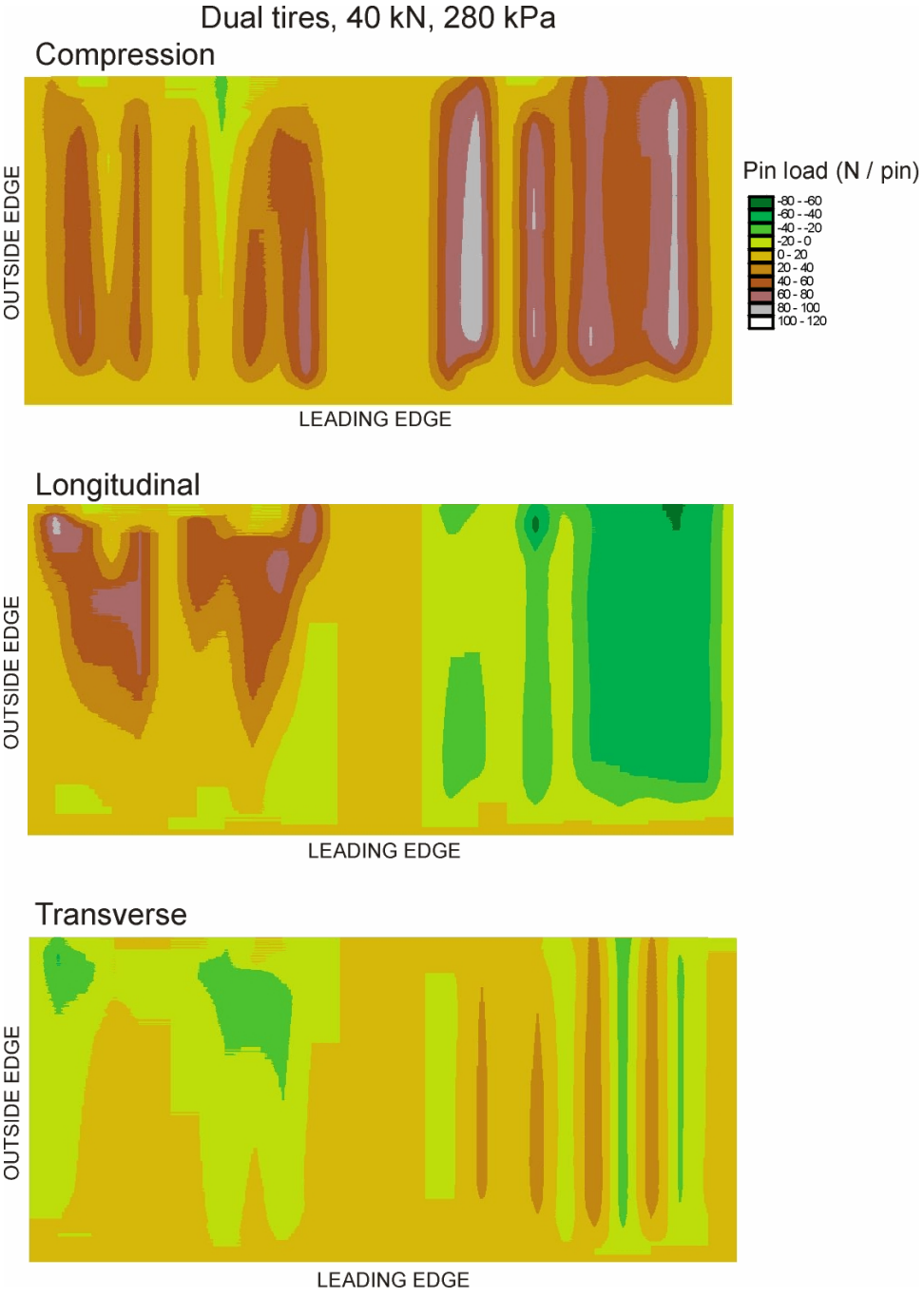

Figure 4.5 Schematic plan view of pin loads for dual tyres: wheel load 40 kN, tyre inflation pressure 280 kPa (not to scale)

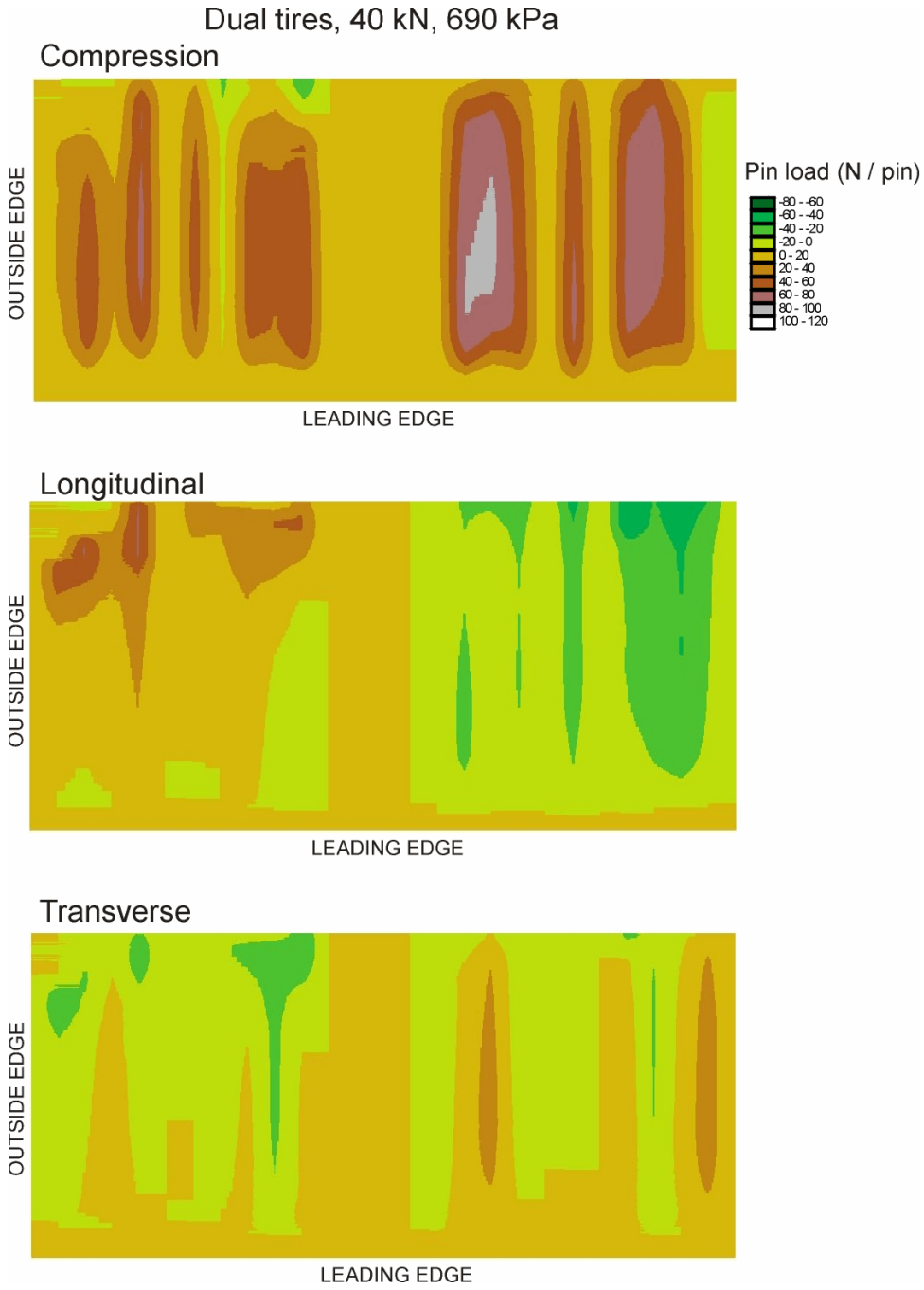

The pin loads recorded depended on whether the individual pin contacted a tyre tread block or happened to fall into a groove in the tread pattern, and the pin loads have been smoothly interpolated between pins. Therefore the pin load patterns shown are somewhat idealised from the real patterns, which would have been much more sharply defined.

Similar plots have been produced for selected dual tyre wheel load and inflation pressures, figures 4.4 and 4.5. The 40kN/690kPa combination is typical of conventional trucks, whereas the 40kN/280kPa combination is typical of the settings trucks using variable tyre inflation systems.

4.2 Discussion of typical results

4.2.1 Contact patch length

The limited data available on the contact patch length agreed with earlier studies and general experience. Contact patches lengthened for increases in wheel load and decreases in inflation pressure. For the four tests conducted, the contact patch length for the single tyre was slightly more sensitive to inflation pressure than wheel load, with an increase of 25 % in the wheel load causing a 9% increase in contact patch length, but a 20% decrease in inflation pressure causing a 6% to 16% increase in contact patch length.

4.2.2 Sensor pin loads as distinct from contact stresses

It is important to make the distinction between real tyre/road contact stresses (kPa) and the measured compressive, longitudinal and transverse pin loads (N/pin). Figures 4.1 to 4.5 show the *forces* the tyres imposed on the pins. The real contact *stresses* are indeterminant: the pins protruded 1mm above the level of the apparatus bed plate over which the tyres ran, the pins shared the stresses imposed by the tyres with the adjacent bed plate surface, and the area of the tyre lifted and supported by each pin cannot be determined. However, the distributions of the loads on the pins are taken as indicative of the real contact stresses.

4.2.3 Single tyres, compressive pin loads

As shown by figure 4.1, the compressive loads on the pins were affected by the inflation pressure and the wheel load. As either increased, the peak compressive pin load increased. The maximum pin load for any of the four combinations of wheel load and inflation pressure tested was of the order of 120N.

4.2.4 Single tyres, longitudinal pin loads

For the single tyre tests, the longitudinal loads on the pins did not follow the S-shaped pattern, running front to back through the tyre contact patch, which had been observed by others (Lippman 1985; Tielking and Roberts 1987; Siegfried 1998; Douglas et al 2000).

Figure 4.2 shows there was a variation of the distribution across the *width* of the contact patch, with loads with a positive sense found towards the outside edge of the contact patch, and loads with a negative sense found towards the inside edge.

Referring to figure 4.6, longitudinal and transverse sensor readings were positive or negative, depending upon which way the tyre pushed the tip of the pin. The direction in which the wheel travelled also needs to be taken into account.

Figure 4.6 Schematic plan view of sensor apparatus

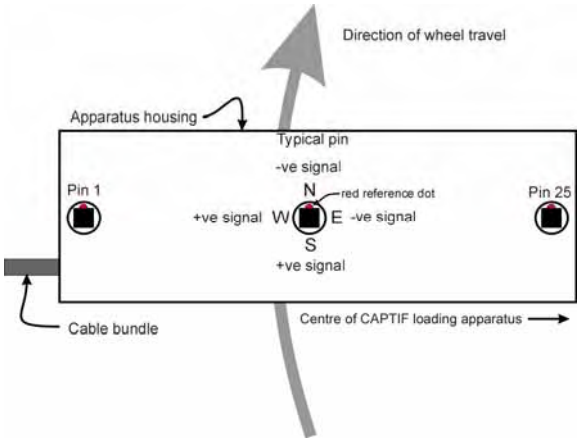

4.2.5 Single tyres, transverse pin loads

Again, as shown in figure 4.3, there was a variation of the pin loads across the width of the tyre contact patch. While there was some inconsistency in the pattern, generally, the transverse pin loads were positive towards the outside edge of the tyre, meaning the pins were pushed toward the outside edge of the tyre. The reverse was true at the inside edge of the tyre. This was the opposite of what has been observed by others (Tielking and Roberts 1987; Douglas et al 2000).

4.2.6 Pin loads for dual tyres

Two sets of pin load data for dual tyres are presented in figures 4.4 and 4.5. The 40kN/690kPa wheel load/tyre inflation pressure combination is typical of real trucks. The 40kN/280kPa combination is typical of the same vehicle employing a reduced tyre inflation pressure setting using a central tyre inflation (CTI) system, where the wheel load remains the same, but the inflation pressure is reduced to obtain the benefits of CTI, such as on an aggregate surfaced road.

In figures 4.4 and 4.5 it can be seen that the compressive pin loads and therefore the tyre loads were mismatched between the inner and outer tyre. Comparing the two figures, it can be seen that deflating the tyres redistributed the compressive pin loads towards the outer edges of both tyres, the expected trend (Marshek et al 1986; De Beer et al 1997).

The longitudinal pin load distribution across the dual tyres mimicked the distribution across single tyres (figure 4.2), with a positive sense towards the outside of the pair of tyres, and a negative sense towards the inside of the pair. Longitudinal pin loads were greater for the lower inflation pressure.

The transverse pin loads under the dual tyres did not follow the trend established by the single tyres. Pin loads generally had a negative sense towards the outside of the pair, and a positive sense towards the inside of the pair. As was the case for the longitudinal pin loads, the transverse pin loads were generally greater for the lower inflation pressure.

4.2.7 Tyre scuffing

The trends and magnitudes of the compression pin loads were as expected for both the single tyres and the dual tyres reported on here. However, the results for the longitudinal and transverse pin loads did not agree with previously-published results.

For the first time to the author's knowledge, contact stress data was reported for tests carried out on a circular track, rather than a linear test facility. Even though the radius of the test arms at CAPTIF is large, at 9m, there still is the possibility of tyre scuffing caused by the continuous right-hand bend the tyres are negotiating. In addition, there are issues of vertical tyre load sharing, and the camber and effective toe-in (or 'toe-out') that must exist. The tyres may be under- or over-steering for the continuous bend in their path, thus causing differences in the longitudinal and transverse pin loads compared with what has been observed by others working on linear facilities with near-perfect wheel alignment.

There was the possibility that a blunder had been made in the processing of the data.

The graphs of pin load distribution are the products of a long series of steps, and their results are a function of a list of interacting inputs, including:

- the arrangement of the strain gauges installed on the pins
- the arrangement of the pins in the apparatus
- the polarity of the wiring
- the direction convention adopted
- the calibration procedure
- the calibration coefficients
- the direction of the wheel travel on the track
- the particular details of a number of spreadsheets used in the analysis of the data
- the particular details of the software used to plot the results.

All were carefully checked through again. Time was invested in an ad hoc experiment, where a car tyre was run in a straight line over the test apparatus again (see figure 1.1). No blunder was found, and the *ad hoc* experiment produced the results seen in the literature for straight-line tests. Thus the unusual results were attributed to tyre scuffing from negotiating the radius of the track, combined with wheel camber and toe-in /toe-out.

4.2.8 Experience with past testing at CAPTIF

The unusual longitudinal and transverse values were not unexpected: the CAPTIF test rig was originally equipped with a slip ring device between the inner and outer wheels on the dual tyre to allow the tyres to turn at different speeds. Eventually it was removed as it was not overly practical and it was found that not using it did not appear to affect road test results.

Earlier tests on chip seals showed that the effects of tyre scuffing were not noticeable when using single tyres to study road texture loss. Tests on sensitive surfaces such as open-graded porous asphalts have also suggested that the effect was not noticeable when dual wheels were used to study fatigue in thin pavement surfaces: no unusual fretting of the surface or fatigue were seen.

4.3 Conclusions about typical results

The measured compressive pin load distributions, indicative of compressive contact stresses, were as expected compared with previous experiments. Peak compressive pin loads increased for increased wheel loads and inflation pressures. For dual tyres at the lowest inflation pressure, compressive pin

loads were greater towards the inner and outer tyre edges. Compressive loads were not shared equally by the two tyres.

Measured longitudinal and transverse pin results did not agree with what has been reported in the literature. These different results may be explained by wheel camber in the CAPTIF rig and by tyre scuffing caused as the tyres negotiated the circular test track, under- or over-steering the curve.

5 Numerical modelling techniques

The second project objective was to use the measured contact stresses in numerical models of pavement response and performance – to test for the significance of using real stresses rather than idealised stresses. A comparison of runs of a finite element numerical model was made using (1) a uniformly distributed vertical pressure acting on a rectangular area of the pavement surface and (2) the measured loads recorded by the apparatus' sensing pins, as inputs. Pavement *response* was predicted for these two loading cases in terms of elastic pavement stresses, strains and surface displacements. Pavement *performance* was examined through the use of a numerical model of rutting for the two loading cases.

A pavement design typical of New Zealand conditions was used for the comparison. The pavement consisted of a 40mm thick non-structural layer of asphalt overlying an unbound granular base 300mm thick, in turn lying on the subgrade.

Full treatment of the numerical modelling is provided in an internal report written for the project and which is located in the appendix.

5.1 Preparation of raw data

The data acquisition routine used resulted in numerous traces for the same loading condition on each pin. Four pins were monitored at a time, all four for compression, and the middle two for longitudinal and transverse loading. Five replicates were made for a group of four pins, then the pins were indexed by one pin, and the next five replicates recorded for that next group of four pins, ie pins 1, 2, 3 and 4 were monitored for five replicates, then pins 2, 3, 4, 5 and so on. All traces for each pin load direction (compression, longitudinal loading, transverse loading) were viewed and a representative single trace selected by inspection. The data for a given pin loading direction (compression, longitudinal loading or transverse loading) was then used to populate a single spreadsheet for each wheel load configuration (single or dual tyre, inflation pressure) and each pin loading type (compression, longitudinal loading or transverse loading). These are the spreadsheets provided on public web site. Data is presented as pin loading in N/pin, having been converted from the output Wheatstone bridge voltages through the calibration coefficients for each pin and direction.

An example of the prepared pin load data is given in figure 5.1.

5.2 Pavement response: comparison of pavement displacements, stresses and strains

For a detailed investigation of the pavement response, a three-dimensional finite element model called ReFEM (Oeser 2004) was used. The program employs special 20-node isoparametric elements, with 60 degrees of freedom and tri-quadratic displacement shape functions. The modelled contact stresses were applied as element forces.

Figure 5.1 Recorded vertical pin loadings (single tyre, 40kN wheel load, 690kPa inflation pressure)

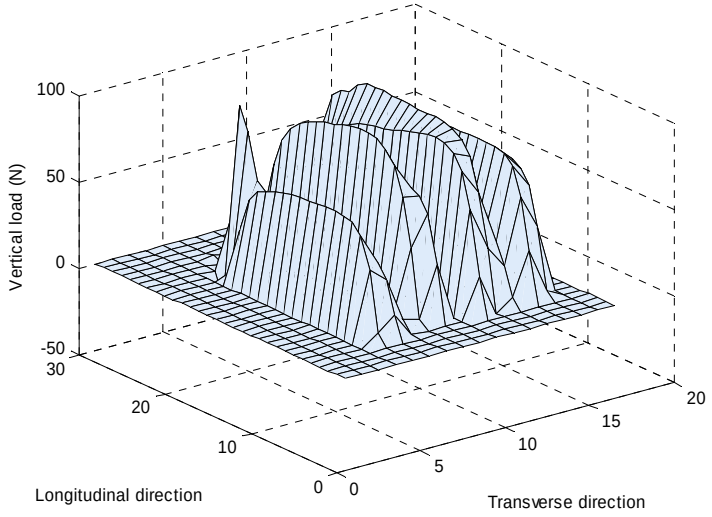

Details of the finite element mesh generated for the problem are given in table 5.1. The plan view of the meshes for the single and dual tyres are shown in figure 5.2 .

Table 5.1 Pavement layer thicknesses and corresponding FEM mesh details

Asphalt layer		Granular base layer		Subgrade	
Thickness (mm)	**No. of elements in the vertical direction**	**Thickness (mm)**	**No. of elements in the vertical direction**	**Thickness (mm)**	**No. of elements in the vertical direction**
40	2	300	4 (single tyre) 3 (dual tyre)	1000	2 (single tyre) 3 (dual tyre)

Figure 5.2 Schematic plan view of FEM meshes for (left) single tyres and (right) dual tyres. Shaded zones indicate tyre contact patch(es)

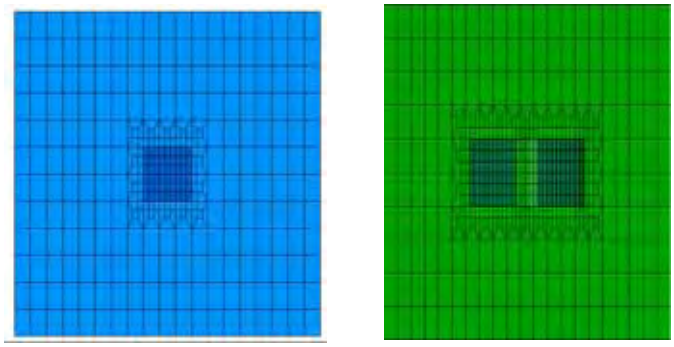

For the comparison of the results of the two loading cases, the uniform pressure integrated over the contact area was assumed to amount to the same vertical force as the wheel load for each test configuration, and to act on a rectangle with the dimensions in table 5.2. Tyre contact patch widths and lengths were derived from the pin load records.

Table 5.2 Details of uniformly distributed loading

Test designation (a)	Tyre contact patch dimensions		Uniformly distributed vertical pressure (kPa)
	width (mm)	length (mm)	
S40550	250	330	480
S40690		310	510
S50550		360	550
S50690	275	310	590
D40280	250	370	220
D40690		280	290
D50280		410	250
D50690	275	300	300

(a) Test designation: 'S' – single tyre, 'D' – dual tyre; next two digits indicate wheel load in kN; last three digits indicate tyre inflation pressure in kPa

The data record for single tyres usually included traces for 11 pins. For the dual tyres, it was usually 25 pins. The loaded area of the FEM meshes included 6 × 9 (lengthwise × widthwise) elements for single tyres, and 2 × 6 × 10 (areas × lengthwise × widthwise) elements for the dual tyres. The FEM meshes were loaded with uniform forces calculated from the average pin load distributed over each FEM mesh element within the loaded area. The plot for a typical modelled loading is shown in figure 5.3.

Figure 5.3 Modelled vertical stress for single tyre, 40 kN wheel load, 690 kPa inflation pressure

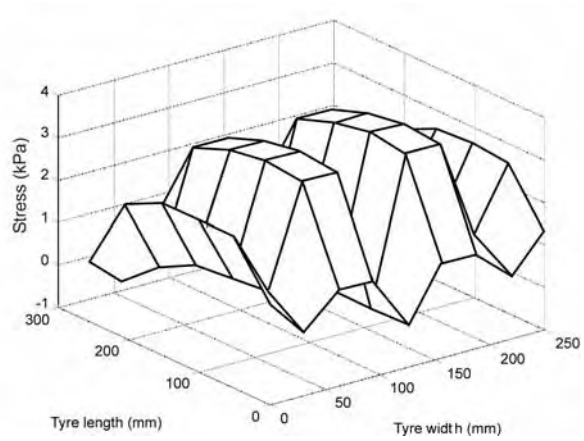

It is important to note that these modelled stresses were the ones used in the FEM modelling, *not* strictly the precise, recorded sensor pin loadings. This idealisation was unavoidable, given the constraints inherent in the FEM program (for example, numbers of elements).

5.3 Material models

5.3.1 Asphalt

The asphalt surface layer was treated as linearly elastic, with Young's modulus E = 3,000 MPa and Poisson's ratio v = 0.35 assumed.

5.3.2 Base course

A non-linear model of unbound granular base course behaviour, under development at the Technische Universitaet Dresden using parameters typical of New Zealand base courses, was employed in the FEM modelling. Full details are given in section 3.2.2 of the internal report presented in the appendix.

5.3.3 Subgrade

The subgrade was modelled as linearly elastic, with Young's modulus E = 70 MPa and Poisson's ratio v = 0.40 assumed.

5.4 Pavement performance: road rutting model

Werkmeister (2007) has developed a procedure for estimating long-term rutting performance based on repeated load triaxial tests (RLT) carried out on samples of base course material and calculated elastic pavement strains. The pavement's conceptual performance history is divided into the 'initial post construction compaction phase', during which the first 25,000 to 100,000 passes of traffic compacts, and therefore ruts the base layer, and the 'steady state' phase during which plastic strain and therefore rutting increase with the remainder of the traffic to which the road is subjected. Relations have been developed to:

- predict the number of passes required to reach the end of the initial post construction compaction phase
- use calculated elastic pavement strains and RLT elastic strain rates to predict the rutting expected during the initial post construction compaction phase
- use calculated elastic pavement strains and RLT elastic strain rates to predict the rutting expected during the subsequent steady state phase.

The routine was applied to data gleaned from RLT tests carried out on a typical New Zealand base course aggregate (greywacke aggregate from Pound's Road quarry in Christchurch, New Zealand) and calculated pavement strains for (a) the uniform vertical pressure loading case, and (b) corresponding loading cases where the modelled non-uniform contact stresses were used. The two sets of predicted rut depths were compared to see if using the 'real' stresses resulted in a difference in the predicted pavement performance.

6 Modelling results and discussion

A full treatment is given in the internal report provided in the appendix. A sample of the results obtained is provided here, generally restricted to single and dual tyres with a wheel load of 40kN and an inflation pressure 690kPa. Comparisons are made between the calculated results for the uniformly distributed pressure loading case and the loading case using the modelled non-uniform contact stresses.

6.1 Results: vertical stresses, vertical strains, vertical pavement surface displacements

Figure 6.1 shows the comparison of vertical stresses in the transverse plane, under a single tyre, when the uniform vertical pressure is applied on the pavement surface, and when the full set of non-uniform stresses is applied. In the latter case, the effect of the stress concentrations under the tyre ribs is clear. For a given depth in the base layer, the vertical stress is slightly greater.

Figure 6.1 Vertical pavement stresses from the pavement surface downwards, in the transverse plane for a single tyre, 40 kN wheel load, 690 kPa inflation pressure – for uniform contact pressure (left) and modelled vertical, transverse and longitudinal contact stresses (right)

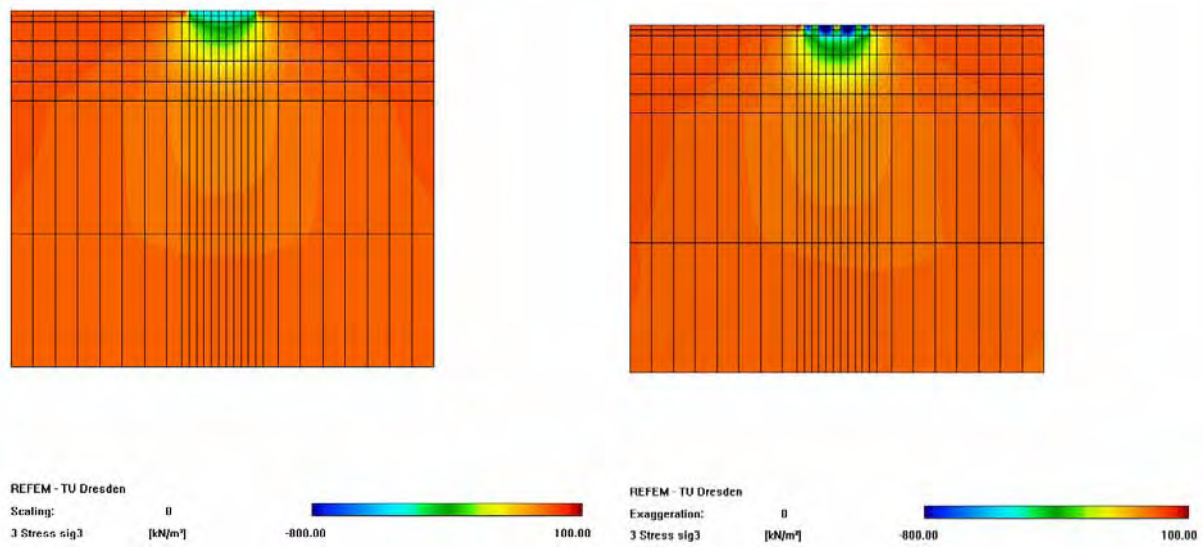

An interesting comparison is made on figure 6.2 for dual tyres. While the concentration of stress due to the tyre ribs is again evident, it is also clear that the two tyres in the dual arrangement were carrying unequal loads. The combined effect is to increase the vertical stress in the base significantly when compared with the calculations for the uniform pressure loading case where the tyre loads are equal, and to generate asymmetrical stresses.

Figure 6.2 Vertical pavement stresses from the pavement surface downwards, in the transverse plane for dual tyres, 40kN wheel load, 690kPa inflation pressure – for uniform contact pressure (left) and modelled vertical, transverse and longitudinal contact stresses (right)

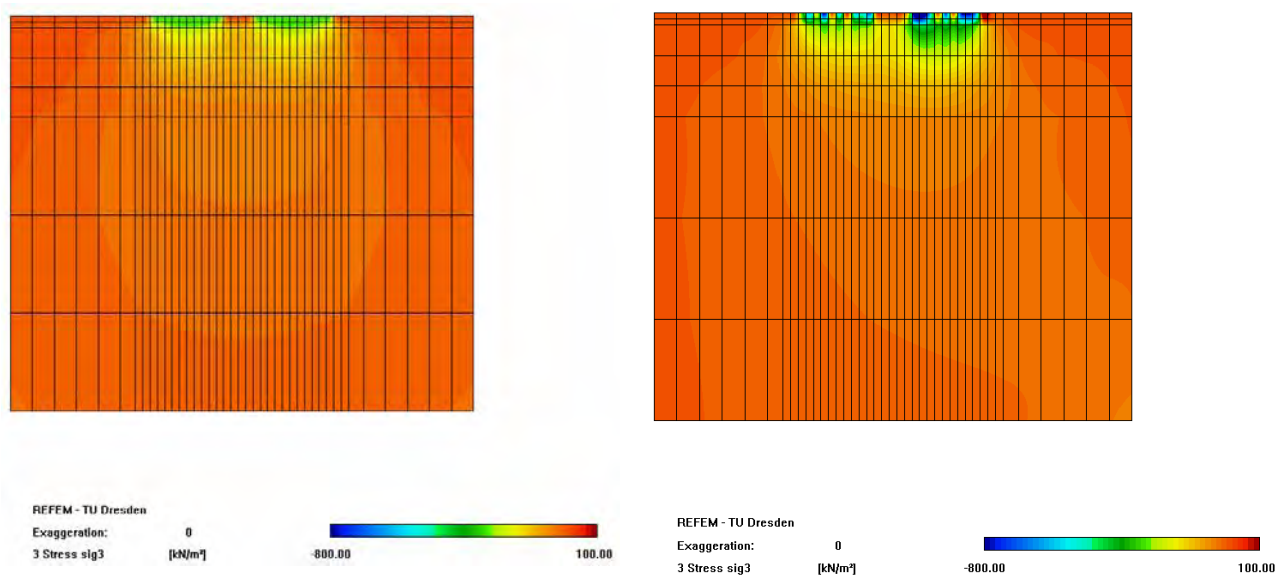

Other plots (see the appendix) indicate that for single tyres, the vertical stress calculated under the centre of the tyre at the top of the subgrade can be as much as 3% to 8% greater for the non-uniform stresses, compared with the uniform surface pressure case, for the configurations considered (S40550, S40690, S50550, S50690). For the dual tyres, the corresponding increase ranged from 12% to 27% (for D40280, D40690, D50280, D50690).

For single tyres, calculated base strains were greater for the non-uniform contact stress case (figure 6.3), compared with those for the uniform surface pressure case. The strains were more intense under the tyre and they penetrated more deeply.

Figure 6.3 Vertical elastic pavement strains from the pavement surface downwards, in the transverse plane for a single tyre, 40kN wheel load, 690kPa inflation pressure – for uniform contact pressure (left) and modelled vertical, transverse and longitudinal contact stresses (right)

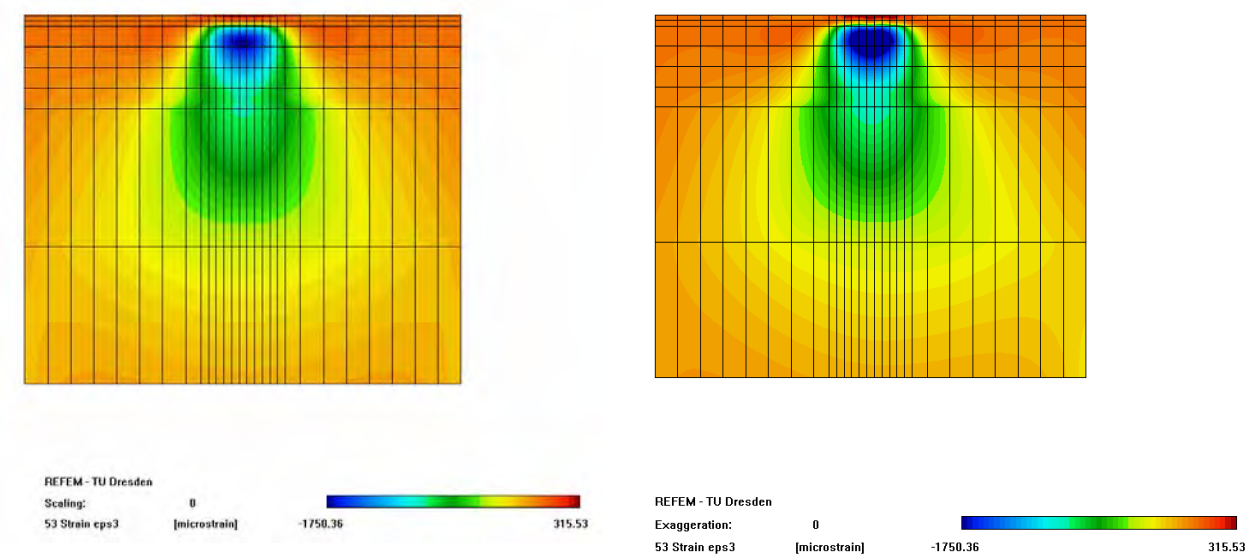

Again, the unequal loading of the dual tyres was reflected in the vertical strain distribution (figure 6.4). Strains were more intense under the more heavily loaded tyre. The strains were slightly asymmetrical in the subgrade as well, although the difference did not appear great, when compared with the uniform pressure case.

Figure 6.4 Vertical elastic pavement strains from the pavement surface downwards, in the transverse plane for dual tyres, 40kN wheel load, 690kPa inflation pressure – for uniform contact pressure (left) and modelled vertical, transverse and longitudinal contact stresses (right)

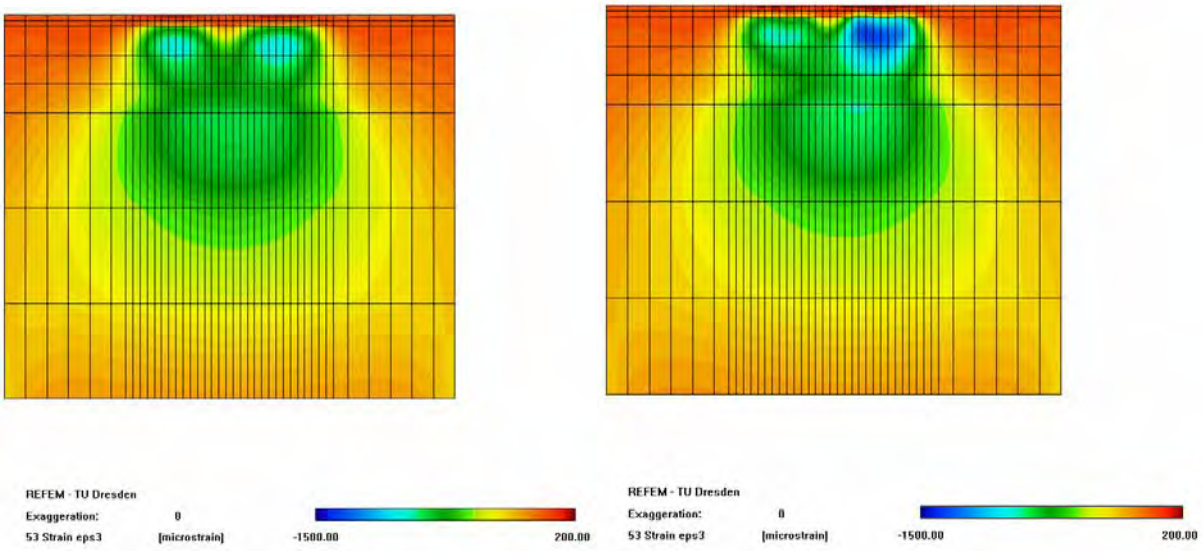

The peak base strains occurred at about 1/3 of the base depth below the top of the base layer. Plots given in the appendix indicate that peak strains calculated for the non-uniform contact stress distribution were 16% to 20% greater than those calculated for the uniformly distributed pressure

loading case, for the single tyre configurations studied ((S40550, S40690, S50550, S50690). For the dual tyres, they were 32% to 55% greater (for D40280, D40690, D50280, D50690).

The vertical elastic strains, integrated with depth, give the elastic pavement surface deflections. These are shown for single tyres on figure 6.5. The effect of the non-uniform vertical stress and the surface shears (longitudinal and transverse) – the tyre scuffing discussed earlier – have given rise to an asymmetrical pavement surface deflections for the modelled pavement surface stresses. The deflection bowl appears to be broader, too.

Figure 6.5 Vertical elastic pavement deflection for a single tyre, 40kN wheel load, 690kPa inflation pressure – for uniform contact pressure (left) and modelled vertical, transverse and longitudinal contact stresses (right)

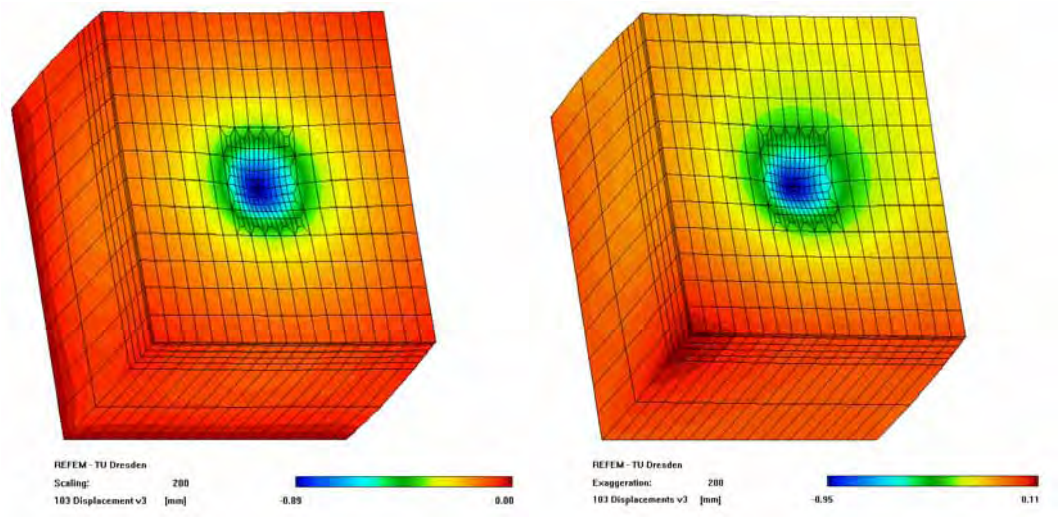

Turning to the dual tyres, evidence of the unequal tyre loading is again observed (figure 6.6). It appears that with the stress concentrated under the tyre ribs, the pavement deflections are actually slightly less at distance, for the non-uniform stress case.

Figure 6.6 Vertical elastic pavement deflection for dual tyres, 40kN wheel load, 690kPa inflation pressure – for uniform contact pressure (left) and modelled vertical, transverse and longitudinal contact stresses (right)

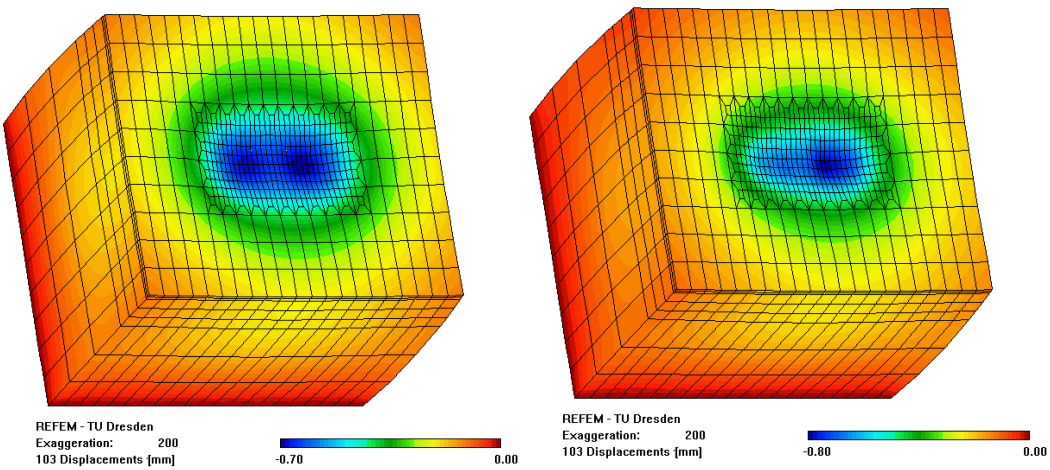

Vertical pavement surface deflections are further compared for the two loading cases on figure 6.7. For the single tyre configurations shown, centreline deflections calculated for the non-uniform contact stress distributions were 5% to 8% greater than those calculated for the uniform contact pressure.

Figure 6.7 Elastic pavement deflections in the transverse plane for single and dual tyres, 40 and 50kN wheel loads, 550 and 690kPa inflation pressures

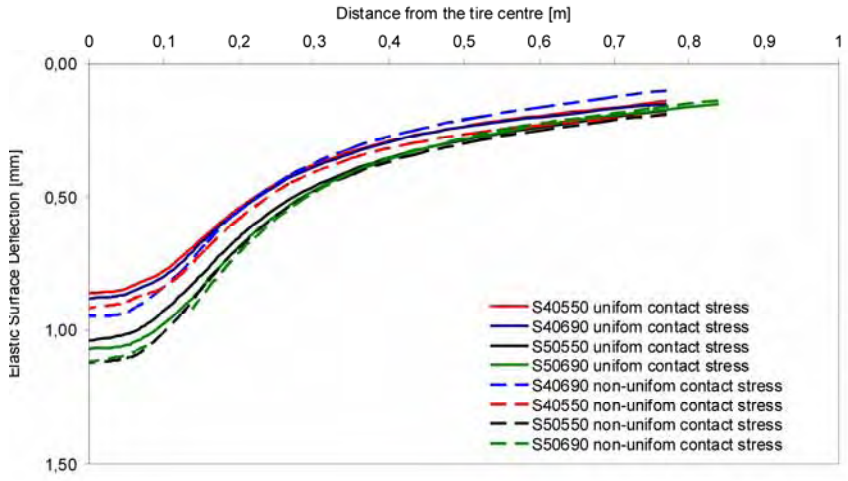

.

6.2 Shear strains in the longitudinal plane

Given the impact of shear strains on granular material behaviour and the fore-and-aft nature of the effects of traction on the road structure, the shear strains in the *longitudinal* plane were plotted (figure 6.8, single tyres; figure 6.9, dual tyres). There is an increase in shear strains, and the strains become somewhat asymmetrical front to back, when the non-uniform contact stresses are input, compared to the uniform vertical pressure, but the differences do not appear great.

Figure 6.8 Fore-and-aft elastic pavement shear strains from the pavement surface downwards, *in the longitudinal plane*, for a single tyre, 40kN wheel load, 690kPa inflation pressure – for uniform contact pressure (left) and modelled vertical, transverse and longitudinal contact stresses (right)

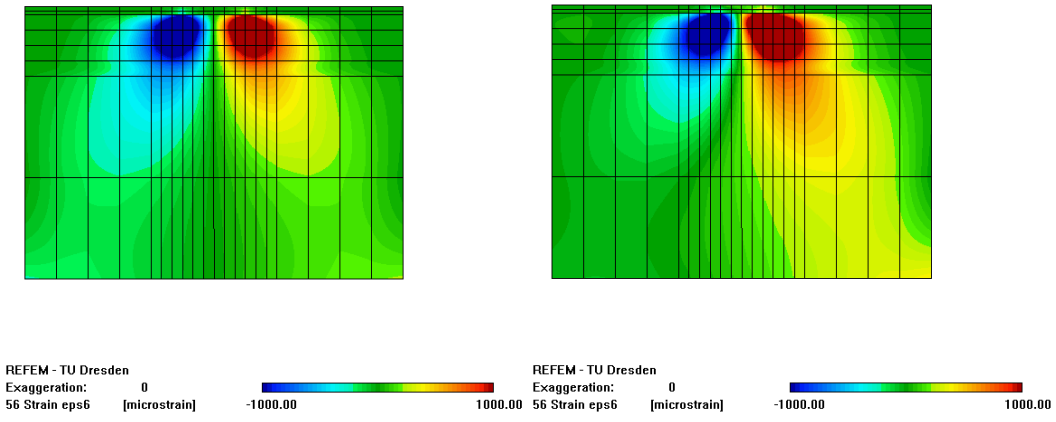

Figure 6.9 Fore-and-aft elastic pavement shear strains from the pavement surface downwards, *in the longitudinal plane*, for dual tyres, 40kN wheel load, 690kPa inflation pressure – for uniform contact pressure (left) and modelled vertical, transverse and longitudinal contact stresses (right)

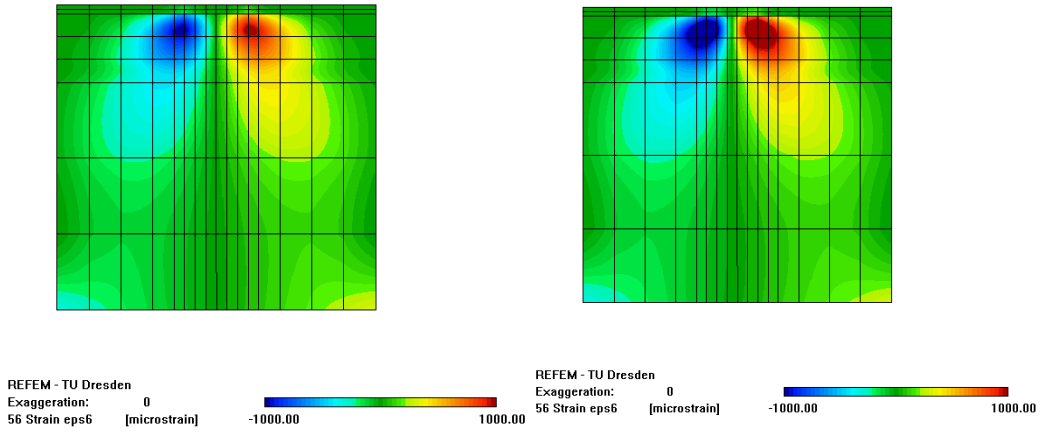

6.3 Rut development

The rut development model described in section 5.4 was applied to the eight configurations studied (single tyres S40550, S40690, S50550, and S50690, and dual tyres D40280, D40690, D50280, D50690). Rut development was predicted for 1 million passes using the calculations for the non-uniform contact patch stresses, and plotted against the ruts predicted for the uniform vertical pressure. Thus the method of predicting rut development was the same for both loading cases: the difference was the contact patch stresses used in the calculations. Results are shown in figure 6.10.

Figure 6.10 Comparison of rut development predicted from uniform and non-uniform contact stresses

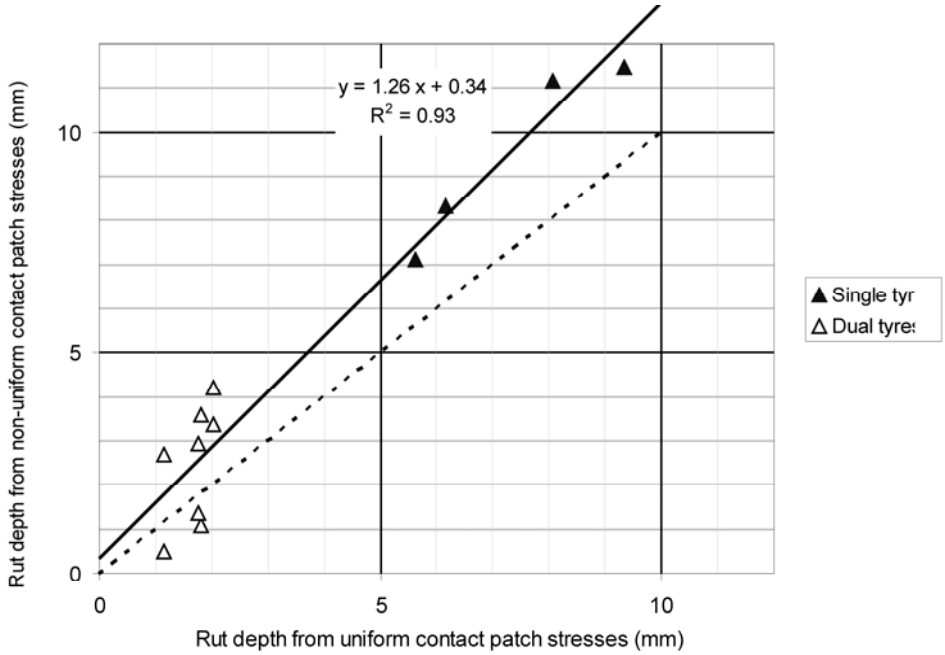

Individual rut depths have been plotted for both tyres in a dual set, because the loads were not equal on the two tyres.

It can be seen in the figure that the rut depths predicted by Werkmeister's method are about 26% greater when the calculations are made on the basis of the modelled non-uniform contact stresses, when compared with the calculations based on uniform contact pressures.

6.4 Discussion of results

Discussion is based on the results of the tests performed at CAPTIF and the pavement layer model used in the FEM analysis. They should not be generalised to real pavements.

The second and third project objectives concerned the use of the measured contact stresses in models of pavement response and performance, to see if differences arose in those models' predictions, compared with what would be predicted on the basis of the more conventional uniform contact pressures. Predicted pavement response was examined in terms of elastic pavement stresses, strains, and displacements. Pavement performance was predicted in terms of rut depth development.

As seen on the figures presented, there were differences in response, but they were often not large. Vertical stresses on top of the subgrade were 3% to 8% greater when the non-uniform contact stresses were used. For dual tyres, the differences were greater at 12% to 27%, but the larger differences may well have been due to the unequal loading of the two tyres in the dual. Peak base strains, occurring about 1/3 below the top of the base layer, were 16% to 20% more for single tyres when the non-uniform contact stresses were input, and 32% to 55% more for the dual tyres, but again, the unequal tyre loading would have affected the calculated difference. Centreline elastic surface deflections were 5% to 8% greater for single tyres when the non-uniform contact stresses were input, in agreement with the increase in the vertical stresses on the top of the subgrade.

These differences in *response,* though not particularly great, especially if some credit is given to the unequal tyre loads in the dual tyre configurations, were enough however to affect pavement *performance* significantly. The rut depths predicted using the non-uniform contact stresses were a little over a quarter greater than those predicted using the conventional uniform pressure. It this translates into a quarter shorter pavement design life, then the implication is serious, from a practical pavement management point of view. A pavement thought to have a design life, of, say, 17 years, would only last about 13.

Such predictions are limited by many factors, including:

- the impacts of the tyre scuffing on the measured sensing apparatus pin loads
- the selection of the representative trace for each pin
- the modelling of the 'real' contact stresses that was necessary to input them to the finite element model
- the modelling of pavement stresses and strains in the finite element model
- the assumptions in Werkmeister's rutting model
- the limitation of the results to the eight configurations studied.

However, it is felt that there is enough evidence in the experimental results to conclude that there are small though measurable differences in pavement response when modelled using non-uniform contact stresses, and that these differences in pavement response give rise to significant differences in

predicted pavement performance. There is ample justification for using more realistic contact stresses in models of pavement response and performance.

7 Conclusions

Based on the results of the research, the assumptions made in it, and its limitations, the following are concluded:

- The project's success, or lack of it, in achieving the original objectives, is outlined in table 7.1.

Table 7.1 Project objectives

Objective	Remarks
1 Measure the contact stresses imposed by various tyre types, inflation pressures, and wheel configurations, to identify the more benign combinations, particularly with reference to their use on thin seals and thin asphalt pavements.	**Not achieved**. The scuffing effects, thought to be caused by the camber and/or effective under- or over-steering taking place on the circular test track confounded the results, and made it impossible to validly compare the effects of the tyre types, configurations, wheel loads, and inflation pressures used.
2 Use the measured data in numerical models of the response of pavements.	**Achieved**.
3 Use the measured data in analyses of the rutting of pavements.	**Achieved**.
4 Support existing research into the scuffing effects of various axle combinations which currently relies on tyre forces as inputs, and could benefit from the measurement of contact stress distributions.	**Not achieved.** To carry out such research properly came to be seen to be beyond the scope of the project, however, a much clearer vision of what would be needed to properly address such research has been gained – see Further Research section.

- A practical, reliable apparatus and data-logging system was fabricated. The apparatus provided stable outputs.
- Some of the pin load data was at variance with what has been presented in the literature. These differences were attributed to lateral scuffing that would occur as the wheel assemblies negotiated the constant circular curve of the test track. This effect obscured hoped-for results, but also led to a much clearer understanding of the interaction between tyres and road surfaces, as influenced by suspension geometry (camber, and toe-in or 'toe-out' resulting in an effective under- or over-steering).
- There is enough evidence in the experimental results to conclude that there are small though measurable differences in pavement response when modelled using non-uniform contact stresses, and that these differences in pavement response give rise to significant differences in pavement performance. There is ample justification for using more realistic contact stresses in models of pavement response and performance.

8 Further research

It would be useful to carry out an experimental programme using the apparatus in a linear, full-scale load testing facility, to extend what is available now in the literature. The full suite of results should be made publicly available. It would be fruitful to achieve the objective of identifying the more benign wheel and tyre configurations, especially with their use on the thin asphalt pavements typical of New Zealand.

The project's 'problem' of tyre scuffing could be pursued to advantage:

- Studying scuffing itself related to the fourth objective. Tests could be run in a linear full-scale load test facility, with the wheel aligned with deliberate camber and/or toe-in, set at various values, to examine the effect of scuffing. This would extend the literature, where previous testing has been designed to use tyres with zero camber and zero toe-in to deliberately *avoid* the influences of these effects. The objective of the research would be to measure the surface shear stresses detrimental to pavement performance.
- The apparatus could be employed to attempt to adjust the suspension of the SLAVE units at CAPTIF to eliminate scuffing effects on test pavements.

The numerical models used in the current research were promising. They should continue to be developed, for example, relaxing the data-input constraints, or further calibrating the rutting predictions.

The apparatus' data logging capability could be upgraded. It was seen that there was a mismatch in the resolution of the data along the wheel path and across it. The speed of data capture – determining the resolution of data along the wheel path – could be reduced without impairing the quality of the data but freeing up data-logging capacity for more readings across the wheel path, improving the resolution in that direction. More pins, more closely spaced across the wheel path would improve crosswise data resolution.

With the rapid development of electronics in general, sensing techniques other than the use of electrical resistance strain gauges should be investigated.

9 Public web site

A public web site which contains all the recorded data in Excel spreadsheet format has been posted. The direct link is www.golder.com/Contact_Stress_Study

This report should be read before downloading the files.

10 References

American Society for Testing and Materials (ASTM) (1985) The tire pavement interface. *Proceedings of a symposium sponsored by ASTM Committees E-17 on Travelled Surface Characteristics and F-9 on Tires*, Columbus, Ohio, 5–6 June 1985. Philadelphia, Pennsylvania: ASTM.

De Beer, M, C Fisher and FJ Jooste (1997) Determination of pneumatic tyre/pavement interface contact stresses under moving loads with some effects on pavements with thin asphalt surfacing layers. *Proceedings of the 8th International Conference on Asphalt Pavements, International Society for Asphalt Pavements*, 8–14 August, Seattle, Wash: 179–227.

Douglas, RA (1997a) Unbound roads trafficked by heavily loaded tyres with low inflation pressure. *Paper 11377. Proceedings of the Institution of Civil Engineers, Transportation* 123, no.8: 163–173.

Douglas, RA (1997b). Heavy load, low tire pressure rutting of unbound granular pavements. *Proceedings of the ASCE Journal of Transportation Engineering*123, no.5: 357–363.

Douglas, RA, WDH Woodward and AR Woodside (2000) Road contact stresses and forces under tires with low inflation pressure. *Canadian Journal of Civil Engineering 27*:1248–1258.

Douglas, RA, WDH Woodward and RJ Rogers (2003) Contact pressures and energies beneath soft tires: modelling effects of central tire inflation-equipped heavy-truck traffic on road surfaces. *Transportation Research Record 1819.* Washington, DC: Transportation Research Board. Pp221–227.

Drakos, CA, R Roque, B Birgisson (2001) Effects of measured tire contact stresses on near-surface rutting. *Transportation Research Record 1764*. Washington, DC: Transportation Research Board. Pp59–69.

Eckels, S. (1929) Distribution of wheel loads through various rubber tires. *Proceedings of the 8th Annual meeting of the High Research Board.* Washington, DC, 13–14 December, 1928. Washington, D.C.: National Research Council, Highway Research Board. Pp192–210.

Howell, WE, SE Perez and WA Volger (1985) Aircraft tire footprint forces. Pp 110–124 in *The tire pavement interface*, *ASTM STP 929*. MG Pottinger and TJ Yager (Eds). Philadelphia: American Society for Testing and Materials.

Lippmann, SA (1985) Effects of tire structure and operating conditions on the distribution of stress between the tread and the road. Pp 91–109 in *The tire pavement interface, ASTM ASP 929*. MG Pottinger and TJ Yager (Eds). Philadelphia: American Society for Testing and Materials.

Liu, GX (1992) The area and stresses of contact between tyres and road surface and their effects on road surface. D.Phil. thesis, Department of Civil Engineering, School of the Built Environment, University of Ulster at Jordanstown, Jordanstown, Northern Ireland.

Machemehl, RB, F Wang and JA Prozzi (2005) Analytical study of effects of truck tire pressure on pavement with measured tire-pavement contact stress data. *Transportation Research Record 1919.* Washington DC: Transportation Research Board. Pp111–120.

Marshek, KM, HH Chen, RB Connell and RW Hudson (1986) Experimental determination of pressure distribution of truck tire-pavement contact. *Transportation Research Record 1070.* Washington DC: Transportation Research Board. Pp9–14.

O'Neil, EW Jr (1969) Measurement of pneumatic tire contact pressure for static loading. M.Sc. thesis, Department of Civil Engineering, North Carolina State University, Raleigh, NC.

Oeser, M (2004) Numerische Simulation des nichtlinearen Verhaltens flexibler mehrschichtiger Verkehrswegebefestigungen (Numerical simulations of the non-linear behaviour of flexible pavements – in German). Ph.D. thesis, University of Technology, Dresden, Germany. 20pp.

Park, D-W, MA Epps and E Masad (2005a) Effects of non-uniform tire contact stresses on pavement response. *ASCE Journal of Transportation Engineering 131,* no.11: 873–879.

Park, D-W, E Fernando and J Leidy (2005b) Evaluation of predicted pavement response with measured tire contact stresses. *Transportation Research Record 1919*. Washington DC: Transportation Research Board. Pp160–170.

Prozzi, JA and R Luo (2005) Quantification of the joint effect of wheel load and tire inflation pressure on pavement response. *Transportation Research Record 1919*. Washington DC: Transportation Research Board. Pp134–141.

Roque, R, LA Myers and B Birgisson (2000) Evaluating measured tire contact stresses to predict pavement response and performance. *Transportation Research Record 1716*. Washington DC: Transportation Research Board. Pp73–81.

Siegfried (1998) The study of contact characteristics between tyre and road surface. D.Phil. thesis, Department of Civil Engineering, University of Ulster at Jordanstown, Jordanstown, Northern Ireland.

Siddharthan, R, N Krishnamenon, M el-Mously and PE Sebaaly (2002) Investigation of tire contact stress distributions on pavement response. *ASCE Journal of Transportation Engineering 128*, no.2: 136.

Siddharthan, R, PE Sebaaly, M El-Desouky, D Strand and D Huft (2005) Heavy off-road vehicle tire-pavement interactions and response. *ASCE Journal of Transportation Engineering 131,* no.3: 239.

Smith, BE, WF Matthes and WF Watson (1990) Measurements of maximum pressure at the soil-tire interface of a rubber-tired skidder. *Paper 90–7534, presented at the 1990 International Winter Meeting of the American Society of Agricultural Engineers*, Chicago, 18–21 December 1990.

Tielking, JT and MA Abraham (1994) Measurement of truck tire footprint pressures. *Transportation Research Record 1435*. Washington DC: Transportation Research Board. Pp92–99.

Tielking, JT and FL Roberts (1987) Tire contact pressure and its effect on pavement strain. *ASCE Journal of Transportation Engineering 113,* no.1: 56–71.

Wang, F and RB Machemehl (2006) Mechanistic-empirical study of effects of truck tire pressure on pavement: measured tire-pavement contact stress data. *Transportation Research Record 1947*. Washington DC: Transportation Research Board. Pp136–145.

Weissman, SL (1999) Influence of tire-pavement contact stress distribution on development of distress mechanisms in pavements. *Transportation Research Record 1655*. Washington DC: Transportation Research Board. Pp161–167.

Werkmeister, S (2007) Prediction of pavement response using accelerated test results of New Zealand's CAPTIF facility. Habilitation, University of Technology, Dresden, Germany.

Woodside, AR, WDH Woodward and Siegfried (1999) The determination of dynamic contact stress. *Paper no. CS5-2, Proceedings of the International Conference on Accelerated Pavement Testing*, Reno, Nevada, 18–20 October 1999.